A RESEARCH PROJECT

ON

COMPUTATIONAL ANALYSIS ON THE EFFECT ON OF BUBBLE CAVITATION ON SHIP PROPELLER USING ANSYS SIMULATION TOOL

PRESENTED TO

DEPARTMENT OF MARINE ENGINEERING

UNIVERSITY OF BENIN

P.M.B 1154 UGBOWO, BENIN CITY

PREPARED BY

ANI PETER IKECHUKWU	**ENG1905468**
AGHO AISOSA COLLINS	**ENG1905463**
ONYIA FAITH CHINWENDU	**ENG1905514**
BIOSE-ONYEMANU EMMANUEL	**ENG1905470**

SUPERVISED BY

DR. H.O EGWARE

IN PARTIAL FULFILMENT OF THE REQUIREMENT FOR THE AWARD OF BACHELOR OF ENGINEERING (B.ENG) IN MARINE ENGINEERING

2024

CERTIFICATION

This is to certify that the research project presented to the Department of Marine Engineering was conducted by Ani Ikechukwu peter, Agho Aisosa Collins, Onyia Faith Chiwendu, Biose-Onyemanu Emmanuel all affiliated with the department of marine engineering, University of Benin, Benin City, Edo state, Nigeria, under the guidance and supervision of Dr. H.O Egware.

---------- ----------

DR. H.O EGWARE DATE

PROJECT SUPERVISOR

---------- ----------

DR. E.G SADJERE DATE

H.O.D

---------- ----------

ENGR. MARTIN OSIKHUEMHE DATE

PROJECT COORDINATOR

DEDICATION

We dedicate this project to God, the source of wisdom, knowledge and understanding, for his enabling support and assistance that allowed us to complete this program successfully and to the entire academic community within the department of marine engineering. We extend our deepest appreciation to our parents for their endless love and support, acknowledging that we have reached this milestone because of their encouragement.

ABSTRACT

Cavitation is a phenomenon that significantly impacts the performance, efficiency, and longevity of ship propellers, often leading to issues such as vibration, noise, erosion, and a reduction in propulsive efficiency. The motivation behind this study stems from the need to better understand the dynamics of cavitation bubbles and their effects on propeller performance to design more efficient and durable marine propulsion systems. As cavitation can cause damage to propeller blades and reduce fuel efficiency, addressing this issue is crucial for the advancement of ship design, particularly in terms of material selection, propeller geometry, and operational strategies. The purpose of this research is to analyze the effect of cavitation-induced bubbles on ship propellers using advanced computational tools, thereby providing insights that could guide future propeller designs and enhance maritime operational efficiency.

To achieve this, the study employs ANSYS simulation tools, specifically its Computational Fluid Dynamics (CFD) module, to model and simulate the behavior of cavitation bubbles in proximity to the propeller. The simulations use a multiphase flow model that includes both the liquid and vapor phases, allowing for the simulation of bubble formation, growth, and collapse under various operating conditions using the vp1304 as the propeller model. The study examines different parameters such as propeller rotational speed, fluid velocity, water temperature, and turbulence levels. The simulation environment is built on realistic physical conditions, using detailed mesh generation to accurately capture the complex flow behavior around the propeller blades. ANSYS Fluent's cavitation model is used to simulate bubble dynamics, with a focus on evaluating pressure distributions, vortex shedding, and velocity gradients.

The results of the simulations reveal that cavitation has a profound effect on the hydrodynamic performance of the propeller. Areas of the propeller subjected to low-pressure conditions were found to experience intense cavitation, leading to significant performance degradation, including thrust loss, decrease in torque, decrease in the overall efficiency of the model. Additionally, the simulations suggest that optimizing propeller blade shape and operating conditions could mitigate the detrimental effects of cavitation. The findings highlight the importance of considering cavitation dynamics during the design phase and provide a roadmap for improving propeller efficiency, reducing cavitation damage, and enhancing the overall performance of marine propulsion systems.

Table of Contents

LIST OF FIGURES

LIST OF TABLES

CHAPTER 1
INTRODUCTION

1.1 BACKGROUND OF THE STUDY

Ship propellers are essential components of the propulsion system of a vessel, responsible for converting the engine's mechanical power into thrust to move the ship through water. Propellers function on the principle of hydrodynamic lift, where rotating blades displace water backward, creating an equal and opposite reaction that propels the vessel forward. In modern ships, propellers are designed to operate efficiently across various conditions and speeds, ensuring optimal fuel consumption and minimal environmental impact.

One of the most critical factors affecting the performance of ship propellers is cavitation, a phenomenon that occurs when the local pressure around the propeller blades drops below the vapor pressure of the water, causing the formation of vapor bubbles. These bubbles can collapse violently when they reach higher pressure areas, generating shockwaves that can erode the surface of the propeller blades and produce noise and vibration (Brennen, 1995).

Cavitation leads to a reduction in propeller efficiency and can result in significant damage to the propeller surface over time, causing material degradation, vibration, and increased maintenance costs. For these reasons, understanding and mitigating cavitation is a major concern in propeller design.

Cavitation has been a subject of extensive research since the early 20th century, with pioneering work by scientists such as Lord Rayleigh, who first described the collapse of cavitation bubbles mathematically (Rayleigh, 1917). Over the decades, researchers have sought to understand the mechanisms of cavitation and its effects on marine propellers through experimental, theoretical, and computational approaches.

Early experimental work by Knapp et al. (1970) involved high-speed photography to observe cavitation bubble dynamics and their collapse. These studies provided foundational insights into the formation and collapse of vapor bubbles and their impact on solid surfaces.

Carlton (2007) conducted experiments on full-scale ship propellers in cavitation tunnels, demonstrating the relationship between cavitation and propeller efficiency, noise, and vibration. His work highlighted the importance of propeller geometry and operational conditions in mitigating cavitation.

Recent experiments by Gaggero et al. (2014) used advanced instrumentation, such as laser Doppler velocimetry (LDV) and pressure sensors, to measure cavitation-induced pressure fluctuations and their effects on propeller performance. These studies emphasized the role of blade shape, pitch, and rotational speed in controlling cavitation.

Brennen (1995) developed theoretical models to describe cavitation bubble dynamics, including the growth and collapse of vapor bubbles. His work laid the groundwork for understanding the physical mechanisms of cavitation and its impact on marine systems.

Computational Fluid Dynamics (CFD) has become a powerful tool for studying cavitation. Studies by Menter (1994) and Schnerr and Sauer (2001) introduced turbulence and cavitation models that enabled the simulation of cavitation phenomena in complex flow fields. These models have been widely adopted in marine engineering to predict cavitation behavior and its effects on propellers.

Recent computational studies by Peters et al. (2018) and Liu (2012) used ANSYS Fluent and other CFD tools to analyze the effects of cavitation on propeller performance and structural integrity. These studies demonstrated the potential of computational methods to optimize propeller design and reduce cavitation-related issues.

Cavitation is not only a technical challenge but also an environmental concern. The collapse of cavitation bubbles generates underwater noise, which can disrupt marine ecosystems and contribute to noise pollution (Ross, 1976). Studies by Gaggero et al. (2014) and Yusvika et al. (2020) have highlighted the need to address cavitation-induced noise in propeller design to meet environmental regulations.

Operational factors, such as ship speed, loading conditions, and water temperature, also influence cavitation. Research by Breslin and Andersen (2010) showed that cavitation is more likely to

occur at higher speeds and under heavy loads, emphasizing the need for adaptive propeller designs.

Despite significant advancements in understanding cavitation, several challenges and gaps remain:

I. Dynamic Cavitation Behavior: The precise dynamics of cavitation under varying operational conditions, such as unsteady flows and off-design conditions, are not fully understood.
II. Material Erosion: The mechanisms of cavitation-induced erosion and their long-term effects on propeller materials require further investigation.
III. Noise Prediction and Mitigation: While computational methods have improved, accurately predicting cavitation-induced noise and developing effective mitigation strategies remain challenging.
IV. Design Optimization: Balancing the trade-offs between propeller efficiency, cavitation resistance, and structural durability is a complex task that requires innovative design approaches.

1.2 STATEMENT OF THE PROBLEM

Bubble cavitation is a critical challenge in the operation of ship propellers, where the formation and collapse of vapor bubbles due to pressure variations in water can lead to performance degradation, material damage, and operational inefficiencies. Cavitation reduces propeller efficiency, increases noise and vibration, and contributes to long-term structural damage, as noted in foundational studies on hydrodynamics and propeller behaviour (Breslin & Andersen, 2010). Despite advancements in marine engineering, there is still limited understanding of the precise dynamics of cavitation under different operational conditions, particularly regarding its impact on noise generation, efficiency loss, and material erosion (Yusvika et al., 2020). These dynamic effects complicate the design of propellers, as they must balance the need for efficiency with resilience to cavitation-related stresses (Peters et al., 2018; Liu, 2012). Addressing these gaps is vital to minimizing maintenance costs, improving fuel efficiency, and mitigating environmental impacts, such as underwater noise pollution (Gaggero et al., 2014). Addressing these multifaceted challenges requires a deeper understanding of the interplay between propeller

geometry, operational environments, and cavitation phenomena. This study will leverage computational techniques to investigate these aspects, aiming to advance propeller designs that are more environmentally sustainable and operationally efficient.

1.3 AIM AND OBJECTIVES OF THE PROJECT

1.3.1 AIM OF THE PROJECT

The aim of the project is to carry out computational analysis of the effect of bubble cavitation on ship propellers using ansys simulation tool.

1.3.2 OBJECTIVES OF THE PROJECT

I. To analyze the impact of bubble cavitation dynamics on the efficiency, structural integrity, and work output of ship propellers.
II. To develop a computational framework for modeling and simulating bubble cavitation under various operational conditions, incorporating factors such as propeller geometry and flow characteristics.
III. To propose operational strategies that reduce the adverse effects of cavitation, enhance propulsion efficiency, and minimize environmental impacts, such as underwater noise pollution.

1.4 SCOPE OF PROJECT

This project investigates the impact of bubble cavitation on the performance of a VP1304 propeller using transient simulations in Ansys Fluent. The study aims to compare propeller behavior in two distinct scenarios: one with cavitation and one without.

1.5 SIGNIFICANCE OF THE PROJECT

The significance of this project lies in its potential to enhance ship propeller performance, reduce operational costs, and promote environmental sustainability. By analyzing bubble cavitation using ANSYS simulation, the study aims to optimize propeller designs to minimize cavitation-induced damage, improving efficiency and durability. This will lead to lower fuel consumption,

reduced maintenance costs, and extended propulsion system lifespan. Additionally, the project contributes to environmental efforts by decreasing underwater noise pollution and reducing carbon emissions through fuel-efficient designs. The findings will support the development of robust, eco-friendly propeller technologies, benefiting both the maritime industry and global sustainability initiatives.

CHAPTER TWO
LITERATURE REVIEW

2.1 INTRODUCTION TO CAVITATION IN MARINE PROPELLERS

Cavitation is a critical phenomenon in marine engineering, particularly concerning the performance and durability of ship propellers. Cavitation occurs when a liquid is subjected to rapid changes in pressure, leading to the formation of vapor bubbles in low-pressure regions. These bubbles collapse violently as they move to higher-pressure areas, releasing intense energy that can damage nearby surfaces (Kumar & Saini, 2020).

In marine propellers, cavitation arises due to the hydrodynamic pressures on the blades as they rotate through water. This phenomenon is not merely a physical curiosity but a significant engineering challenge. The collapse of cavitation bubbles produces localized high-pressure jets that can erode the material of the propeller blades, reducing their efficiency and lifespan (Gupta, Saini, & Verma, 2020). Moreover, cavitation affects the fluid dynamics around the propeller, leading to performance losses and increased fuel consumption (Li, Zhou, & Chen, 2021).

2.1.1 Implications of Cavitation on Propeller Performance, Noise, and Durability

The implications of cavitation extend beyond material erosion:

a. Performance Degradation: Cavitation alters the pressure distribution along the propeller blade surface, reducing thrust and efficiency. Studies indicate that a heavily cavitating propeller may experience a thrust loss of up to 10% (Wang et al 2022).

b. Noise Generation: The collapse of cavitation bubbles produces noise, which is particularly

problematic in military applications where stealth is critical. Additionally, cavitation noise contributes to underwater sound pollution, affecting marine ecosystems (Zhang & Wei, 2021).

c. Durability Challenges: Repeated bubble collapse leads to surface pitting and material fatigue. Over time, this degradation necessitates costly repairs or replacements of propellers, impacting operational costs (Gupta et al 2020).

2.1.2 Overview of Cavitation Mitigation Strategies

Mitigating cavitation is vital for maintaining propeller performance and prolonging service life. Common strategies include:

a. Design Optimization: Advanced computational tools like ANSYS enable engineers to optimize blade geometry, reducing pressure differentials that cause cavitation (Zhang & Wei, 2021).

b. **Material Innovations**: Using materials with high resistance to cavitation erosion, such as titanium alloys or composite materials, helps reduce damage (Chen et al 2022).

c. **Operational Adjustments**: Adjusting ship speed and propeller revolutions can minimize cavitation occurrence under certain conditions (Kumar et al 2023).

d. **Surface Coatings**: Applying anti-cavitation coatings enhances surface hardness and mitigates erosion effects (Liu & Zhao, 2020).

2.2 MECHANISMS OF CAVITATION FORMATION

2.2.1 Types of Cavitation

I. **Vaporous Cavitation**: This type occurs when the local pressure in a liquid drops below the vapor pressure, causing the formation of vapor-filled cavities. These cavities collapse when they move into higher-pressure regions, leading to significant damage (Kumar & Saini, 2020).

II. **Bubble Cavitation**: Bubble cavitation involves the growth and collapse of individual bubbles due to pressure fluctuations. It is often observed in turbulent flow conditions and contributes to noise and erosion (Zhang & Wei, 2021).

III. **Sheet Cavitation**: This form of cavitation manifests as a continuous vapor layer on the surface of the propeller blade. Sheet cavitation significantly affects the lift and drag forces, causing performance losses (Li, et al, 2021).

IV. **Tip Vortex Cavitation**: This type occurs at the tips of propeller blades due to the concentrated vortices formed by rapid rotation. Tip vortex cavitation contributes to noise and efficiency reduction (Wang, et al, 2022).

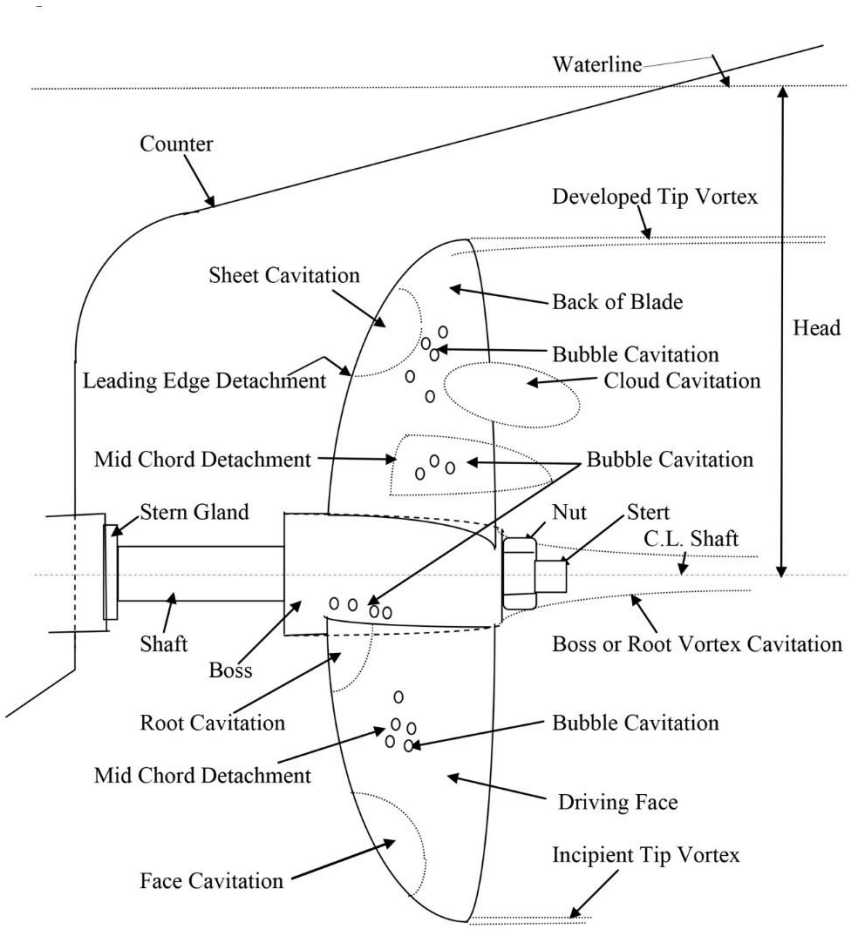

Figure1 Various Types of Cavitation

Figure 2.1: various types of cavitation (Jones and Walker, 2023)

Figure 2.1 efficiently illustrates the fundamental cavitation modes—vaporous, bubble, sheet, and tip vortex—commonly encountered in marine propellers. Although cavitation can occur in multiple forms, the focus of this study is primarily on *bubble cavitation*, with some consideration of tip vortex cavitation in the VP1304 propeller.

2.2.2 Thermodynamic Processes Driving Cavitation

Cavitation is driven by the interplay of thermodynamic factors, including fluid pressure, temperature, and velocity. When a propeller blade rotates, it creates a pressure gradient along its surface. In regions where the pressure drops below the liquid's vapor pressure, bubbles form. As these bubbles collapse, they generate shock waves that erode the material surface (T. Jones and R. Walker, 2023)

The cavitation number (σn) is a dimensionless parameter that quantifies the likelihood of cavitation:

$$\sigma_n = \frac{p_{ref} - P_v}{0.5\rho(nD)^2} \qquad (2.1)$$

Where: p_{ref} is the reference pressure, P_v is the vapor pressure of the fluid, ρ is the fluid density, n is the revolutions per second of the propeller, D is the propeller diameter.

This parameter helps engineers predict and mitigate cavitation by understanding the operating conditions under which it occurs (Wang et al., 2022)

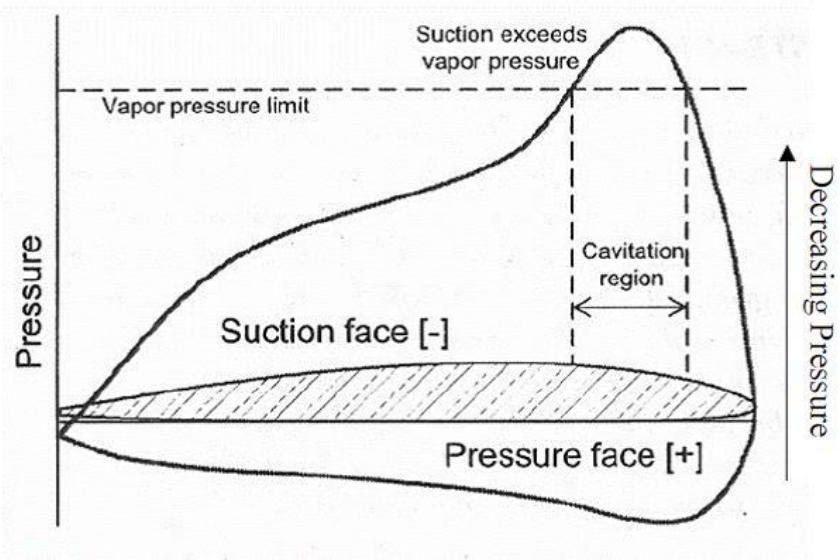

Figure 2.2: pressure distribution and cavitation zones on a propeller blade (Chen et al.,2022)

Figure 2.2 illustrates *how localized low-pressure regions* on a propeller blade can induce cavitation. This study examines how these low-pressure zones form on the leading and/or trailing edges of the VP1304 propeller. This figure sets up an essential link between known cavitation-prone areas and the data generated in CFD simulations. It shows the physical phenomenon expected to replicate numerically where vapor bubbles are most likely to form and collapse highlighting the *practical relevance* of identifying these zones to minimize cavitation damage and performance loss.

2.3 EFFECTS OF CAVITATION ON PROPELLER PERFORMANCE

Cavitation significantly impacts the key performance metrics of propellers:

I. **Thrust Coefficient (K_T)**: The thrust coefficient, defined as: Where T is the thrust force, ρ is the fluid density, n is the revolutions per second, and D is the propeller diameter, measures the effectiveness of the propeller in generating thrust. Cavitation reduces T by altering the flow dynamics around the blade surface (Chen et al., 2022).

Equation for Thrust Coefficient:

$$K_T = \frac{T}{\rho n^2 D^5} \qquad \text{(Chen et al., 2022).} \qquad (2.2)$$

Where T is the thrust force, ρ is the fluid density, n is the revolutions per second, and D is the propeller diameter, measures the effectiveness of the propeller in generating thrust.

K_T is the thrust coefficient

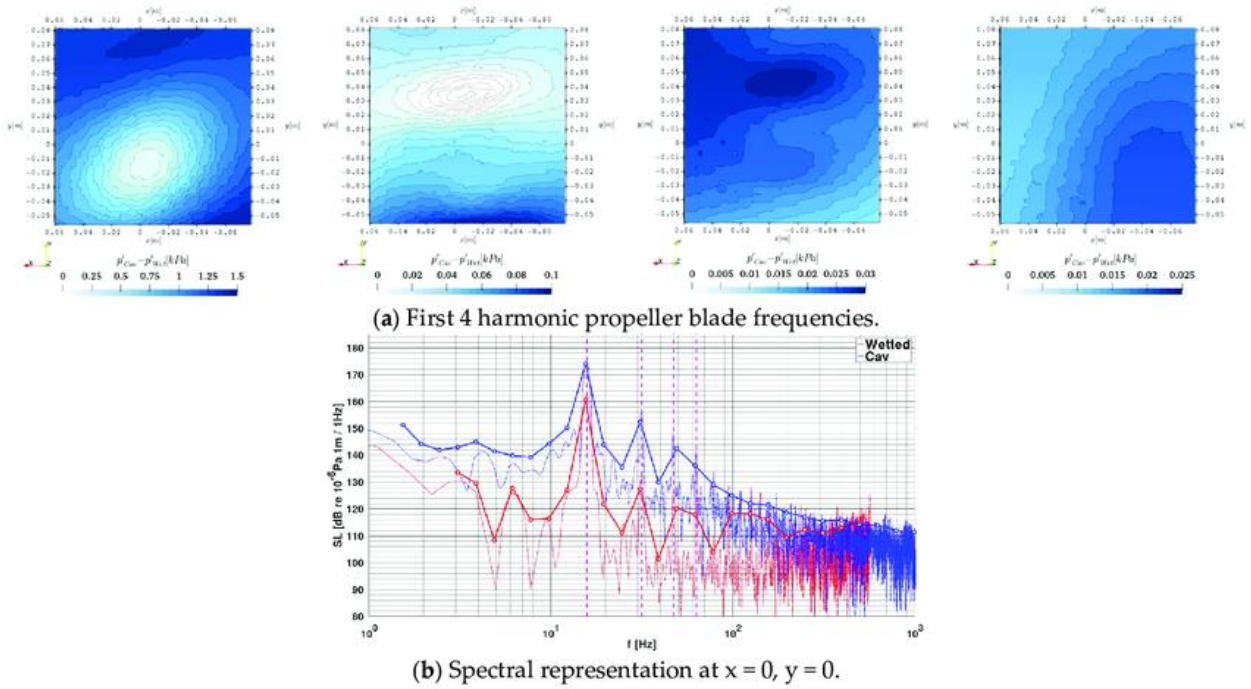

Figure 2.3: comparison of cavitating and non-cavitating propeller performance *(Xin Hai et al., 2022)*

Figure 2.3 presents a comparison of the propeller's overall performance, typically measured in terms of thrust and torque, under both cavitating and non-cavitating conditions. This is relevant to studies analyzing the impact of cavitation on propeller efficiency and the increased risk of erosion. The inclusion of this figure aids observance of the performance reduction caused by cavitation, emphasizing the importance of minimizing or controlling cavitation.

II. **Torque Coefficient (K_Q)**: it is defined as stated in the equation below

Cavitation increases , indicating higher energy losses due to turbulent flows and bubble collapse (Jones and Walker, 2023)

Equation for Torque Coefficient:

$$K_Q = \frac{Q}{\rho n^2 D^5} \quad (2.3)$$

where Q is the torque exerted by the propeller.

2.3.1. Impact on Noise, Vibration, and Material Erosion

a. **Noise**: Cavitation noise results from the collapse of vapor bubbles, producing broadband acoustic emissions. This noise is disruptive to marine life and compromises stealth in naval vessels (Garrison et al,.2023).

b. **Vibration**: The unsteady forces generated by cavitation cause vibrations in the propeller and hull structure, reducing ride comfort and increasing mechanical wear (Wang et al., 2022).

c. **Material Erosion**: The high-energy implosion of cavitation bubbles leads to localized material erosion, creating pits and cracks on the blade surface. This erosion reduces the service life of the propeller (Gupta et al., 2020).

2.4 FLUID PROPERTIES INFLUENCING CAVITATION

Cavitation in marine propellers is strongly influenced by the fluid properties of water, including temperature, density, viscosity, and vapor pressure. Understanding these properties and their interrelationships is critical for predicting cavitation behavior and designing propellers that mitigate its adverse effects.

2.4.1 Effects of Water Temperature, Density, Viscosity, and Vapor Pressure on cavitation

I. **Water Temperature**:

Water temperature significantly impacts cavitation because it influences other fluid properties, such as vapor pressure and viscosity. Higher temperatures increase the vapor pressure of water, lowering the threshold for cavitation onset (Kumar, et al, 2023). For example, at 50°C, water's vapor pressure is approximately 12.3 kPa, compared to 2.3 kPa

at 20°C. This means cavitation is more likely to occur at elevated temperatures, especially in tropical or warm-water operations (Zhang et al ., 2022).

II. **Density (ρ)**:

Density determines the fluid's resistance to cavitation. Lower-density fluids require less pressure drop to initiate cavitation, making them more prone to bubble formation (Li et al., 2021). Saltwater, with a slightly higher density than freshwater, offers marginally greater resistance to cavitation under identical conditions (Chen et al., 2022).

III. **Dynamic Viscosity (μ)**

The viscosity of water affects the energy dissipation in the fluid. Lower viscosity reduces the energy required for cavitation bubble formation. Water viscosity decreases with increasing temperature, further facilitating cavitation at higher temperatures (Brennen, 1995).

IV. **Vapor Pressure (Pv)**

Vapor pressure is the pressure at which water transitions from liquid to vapor at a given temperature. Cavitation occurs when local pressures drop below the vapor pressure. A higher vapor pressure, typically observed at elevated temperatures, reduces the critical pressure differential needed for cavitation onset (Moin & Kim, 1997). This relationship underscores why propellers in warmer waters often experience more severe cavitation compared to colder environments (Wang et al., 2024).

2.4.2 Temperature-Dependent Relationships

The interdependence of temperature, density, dynamic viscosity, and vapor pressure can be mathematically represented and analyzed to predict cavitation thresholds.

Density (ρ): The relationship between density and temperature is shown in Equation 2.4

$$\rho(T) = \rho_0 [1 - \beta (T - T_0)] \quad (2.4)$$

Where:

ρ: Density at temperature T, ρ_0 : Reference density at temperature T_0 , β: Thermal expansion coefficient, T: Temperature, T_0 : Reference temperature

Dynamic Viscosity (μ) Variation with Temperature correlation is expressed in Equation 2.5

$$\mu(T) = \mu_0 e^{-b\,(T-T_0)} \tag{2.5}$$

Where:

μ(T): Viscosity at temperature T, μ_0 : Reference viscosity at temperature T_0, b: Fluid-specific constant, T: Temperature, T_0 : Reference temperature

Saturation Vapor Pressure (P_v) Relationship with Temperature is shown in Equation 2.6

$$In(P_v) = \frac{\Delta H_v}{R}\left(\frac{1}{T_0} - \frac{1}{T}\right) + In(P_{v0}) \tag{2.6}$$

Where:

P_v : Saturation vapor pressure at temperature T, ΔH_v : Enthalpy of vaporization, R: Universal gas constant, P_{v0}: Vapor pressure at reference temperature T_0 , T: Temperature, T_0 : Reference temperature

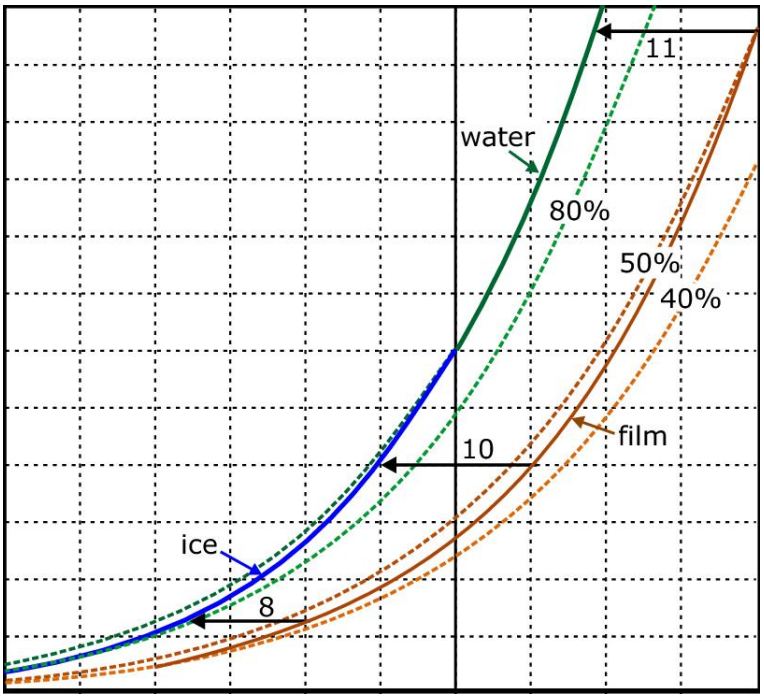

Figure 2.4: variation of water vapor pressure with temperature *(*Padfield and Tim. 2014).

The fluid properties of water play a pivotal role in cavitation dynamics. Temperature affects vapor pressure, viscosity, and density, creating a cascade of effects that influence cavitation onset and severity. By incorporating these relationships into computational models, engineers can design.

The figure above illustrates the relationship between water vapor pressure and temperature, showing how vapor pressure increases as temperature rises. This relationship is fundamental to understanding the onset of cavitation, as higher vapor pressure at elevated temperatures reduces the pressure threshold required for bubble formation. For a study involving temperature-dependent analysis of cavitation, such as within a range of 0°C to 50°C, this figure supports the theoretical background by explaining why cavitation is more likely at higher temperatures.

2.5 NUMERICAL METHODS FOR CAVITATION ANALYSIS

Computational Fluid Dynamics (CFD) has emerged as a pivotal tool in marine engineering, particularly for analyzing the performance of marine propellers and understanding complex fluid interactions. Recent advancements in CFD have significantly enhanced its application in marine environments, allowing for more accurate simulations of fluid flow around submerged bodies, which is crucial for predicting hydrodynamic forces, cavitation phenomena, and overall performance metrics (Smith et al., 2022).

In marine applications, CFD is particularly valuable for studying cavitation, a phenomenon that occurs when local pressure drops below the vapor pressure of the fluid, leading to the formation of vapor bubbles. These bubbles can adversely affect the performance and structural integrity of propellers, causing issues such as erosion, noise, and loss of efficiency (Lee & Zhao, 2019). By employing advanced CFD techniques, researchers can visualize and analyze the flow field, identify cavitation regions, and optimize propeller designs to mitigate cavitation effects (Chang et al., 2023).

2.5.1 Governing Equations

The foundation of any CFD analysis lies in the governing equations that describe fluid motion. For incompressible flow, the primary equations used are the continuity equation and the Navier-Stokes equations (Moin & Kim, 1997).

I. Continuity Equation

The continuity equation ensures the conservation of mass in the fluid flow and is expressed as:

$$\frac{\partial \rho}{\partial t} + \nabla . (\rho u) = 0 \qquad (2.7)$$

where ρ is the fluid density, u is the velocity vector, and t is time.

This equation states that the rate of change of density within a control volume plus the net mass flux out of the volume must equal zero (Moin & Kim, 1997). In the context of cavitation analysis, maintaining mass conservation is crucial, especially when dealing with phase changes between liquid and vapor.

II. Momentum Equation (Navier-Stokes)

The momentum equation, commonly referred to as the Navier-Stokes equation, describes the motion of fluid substances and is given by:

$$\frac{\partial(\rho u)}{\partial t} + \nabla \cdot (\rho u u) = -\nabla P + \nabla \cdot (\mu(\nabla u + (\nabla u)^T)) \qquad (2.8)$$

In this equation, P represents the pressure, and μ is the dynamic viscosity of the fluid.

The left-hand side of the equation accounts for the change in momentum due to time and convective effects, while the right-hand side includes the pressure gradient and viscous forces acting on the fluid (Moin & Kim, 1997; Chen & Wu, 2019).
The Navier-Stokes equations are fundamental for capturing the complex interactions in the flow field around propellers, including the onset of cavitation. Accurate numerical solutions to these equations are essential for predicting the behavior of cavitation bubbles and their impact on propeller performance (Sotiropoulos et al., 2002).

2.6 CAVITATION MODELS IN CFD

2.6.1 Rayleigh-Plesset Equation for Bubble Dynamics

The Rayleigh-Plesset equation is a fundamental equation used to describe the dynamics of spherical gas bubbles in a liquid, particularly in the context of cavitation. This equation captures the balance of forces acting on a bubble and is expressed as follows:

$$R_B \frac{d^2 R_B}{dt^2} + \frac{3}{2}\left(\frac{dR_B}{dt}\right)^2 = \frac{P_v - P}{\rho} \qquad (2.9)$$

where:

R_B is the radius of the bubble, P_v is the pressure inside the bubble, P is the ambient pressure, ρ is the density of the liquid (Plesset & Prosperetti, 1977).

This equation accounts for the inertial effects of the bubble's motion, the pressure difference between the vapor inside the bubble and the surrounding liquid, and the viscous effects that may influence bubble dynamics. The Rayleigh-Plesset equation is crucial for understanding how bubbles grow and collapse in response to changes in pressure, which is particularly relevant in marine applications where cavitation can lead to significant performance issues and structural damage (Rayleigh, 1917 and Plesset, 1949).

2.6.2 Comparison of Mass Transfer Models

In CFD simulations of cavitation, various mass transfer models are employed to accurately represent the phase change between liquid and vapor. Two prominent models are the Schnerr-Sauer model and the Full Cavitation Model (FCM).

I. Schnerr-Sauer Model

The Schnerr-Sauer model is a widely used approach for simulating cavitation in incompressible flows. This model incorporates the effects of mass transfer between the liquid and vapor phases based on the local pressure conditions. The model assumes that the vapor phase can be treated as a compressible fluid, allowing for the calculation of

vapor volume fraction and the dynamics of bubble formation and collapse (Schnerr & Sauer, 2001).

The Schnerr-Sauer model is particularly effective in capturing the onset of cavitation and the subsequent behavior of vapor bubbles in a flow field. It provides a balance between computational efficiency and accuracy, making it suitable for a variety of engineering applications, including marine propeller simulations (Schnerr & Sauer, 2001; Kawai et al., 2004).

II. Full Cavitation Model (FCM)

The Full Cavitation Model (FCM) is a more comprehensive approach that accounts for the detailed physics of cavitation, including the interactions between the liquid and vapor phases. FCM incorporates the effects of turbulence, pressure fluctuations, and bubble dynamics, providing a more accurate representation of cavitation phenomena (Zwart et al., 2004).

This model is particularly useful in scenarios where cavitation is highly dynamic and influenced by complex flow patterns, such as around marine propellers. FCM allows for the simulation of the entire cavitation process, from bubble nucleation to growth and collapse, providing insights into the impact of cavitation on performance metrics like thrust and torque (Zwart et al., 2004; Langtry et al., 2006).

2.7 TURBULENCE MODELS FOR CAVITATION SIMULATION

Turbulence plays a critical role in the dynamics of fluid flow, particularly in the context of cavitation. Accurate modeling of turbulence is essential for predicting the behavior of cavitating flows around marine propellers. Several turbulence models are commonly used in CFD simulations, each with its strengths and limitations.

2.7.1 Standard $k-\epsilon$ Model

The Standard k−ϵ model is one of the most widely used turbulence models in engineering applications. It is a two-equation model that solves for the turbulent kinetic energy (k) and the turbulent dissipation rate (ϵ). The governing equations for the k−ϵ model are given by:

$$\frac{\partial \mathrm{k}}{\partial \mathrm{t}} + U_j \frac{\partial \mathrm{k}}{\partial_{\mathrm{xj}}} = \mathrm{P}_k - \beta^* \rho \mathrm{k} \epsilon \qquad (2.10)$$

where: k is the turbulent kinetic energy, U_j is the velocity vector, P_k is the production of turbulent kinetic energy, $\beta^* \rho \mathrm{k} \epsilon$ is a constant, ρ is the fluid density ,ϵ is the turbulent dissipation rate (Launder & Spalding, 1974).

The Standard k−ϵ model is effective for simulating fully developed turbulent flows but may struggle in predicting flows with strong adverse pressure gradients or separation, which are common in cavitating flows (Katz and Plotkin, 2010)

2.7.2 SST k−ω Model

The Shear Stress Transport (SST) k−ω model combines the advantages of the k−ϵ and k−ω models, providing improved accuracy in boundary layer flows and better performance in adverse pressure gradient situations. The SST k−ω model uses the turbulent kinetic energy (k) and the specific dissipation rate (ω) as its two variables. This model is particularly effective in capturing the effects of turbulence on cavitation dynamics (Launder and Spalding, 1974)

The governing equations for the SST k−ω model include terms for the transport of kkk and ωωω, allowing for a more accurate representation of the turbulent flow field, especially in regions where cavitation occurs (Langtry and Menter, 2009)

$$\frac{\partial \mathrm{k}}{\partial \mathrm{t}} + U_j \frac{\partial \mathrm{k}}{\partial_{\mathrm{xj}}} = \mathrm{P}_k - \beta^* \rho \mathrm{k} \omega + \quad \frac{\partial}{\partial_{\mathrm{xj}}} \left[(\mu + \sigma_{\mathrm{k}} \mu_{\mathrm{t}}) \frac{\partial \mathrm{k}}{\partial_{\mathrm{xj}}} \right]$$

$$\frac{\partial(\rho\omega)}{\partial t} + U_j \frac{\partial(\rho U_j \omega)}{\partial_{xj}} = \frac{\partial}{\partial_{xj}} \left[(\mu + \sigma_\omega \mu_t) \frac{\partial \omega}{\partial_{xj}} \right] + \alpha \frac{\omega}{k} P_k - \beta\rho\omega^2 + P_{wb} \quad (2.11)$$

Transition-Sensitive Models

Transition-sensitive models are designed to capture the transition from laminar to turbulent flow, which is crucial in many applications, including cavitation. These models incorporate additional equations or modifications to existing turbulence models to account for the onset of turbulence due to flow instabilities (Wilcox, 1998). Transition-sensitive models are particularly useful in scenarios where the flow is subject to varying conditions, such as changes in velocity or pressure, which can significantly influence cavitation behavior. By accurately predicting the transition to turbulence, these models can provide better insights into the cavitation process and its effects on performance metrics (Langtry & Menter, 2009).

2.7.3 Importance of Turbulence in Cavitation Simulations

Turbulence significantly influences the behavior of cavitation bubbles and the overall flow field around propellers. The interaction between turbulent eddies and cavitation bubbles can lead to complex flow patterns, affecting bubble dynamics, growth, and collapse (Lee & Moser, 2011). Accurate turbulence modeling is essential for predicting these interactions and understanding their impact on performance metrics such as thrust, torque, and cavitation volume fraction. In cavitation simulations, turbulence models help capture the effects of turbulent fluctuations on pressure fields, which are critical for determining the onset of cavitation. Additionally, turbulence can enhance mixing and energy dissipation in the flow, influencing the stability and dynamics of cavitation bubbles (Menter, 1994). Therefore, selecting an appropriate turbulence model is crucial for achieving reliable and accurate simulation results in cavitation studies.

2.8 VALIDATION OF CFD SIMULATIONS

2.8.1 Role of Experimental Data in Validating Simulations

The validation of Computational Fluid Dynamics (CFD) simulations is a critical step in ensuring the accuracy and reliability of numerical models used in engineering applications, particularly in the study of cavitation and propeller performance. Experimental data serves as a benchmark against which CFD results can be compared, providing a means to assess the fidelity of the simulation models and the assumptions made during the modeling process (Versteeg & Malalasekera, 2007).

Validation involves comparing key performance metrics obtained from CFD simulations, such as thrust and torque coefficients, with experimental measurements. This process helps identify discrepancies between the numerical predictions and physical observations, allowing for adjustments in the simulation parameters, turbulence models, or numerical methods to improve accuracy (Jiang et al., 2010). Furthermore, a well-validated CFD model can enhance confidence in its predictive capabilities for scenarios that may be difficult or impractical to test experimentally (Rodi, 1997).

2.8.2 Potsdam Propeller Test Case (PPTC)

The Potsdam Propeller Test Case (PPTC) is a widely recognized benchmark for validating CFD simulations of marine propellers. This case study involves a series of experiments conducted at the Potsdam Institute for Climate Impact Research, where detailed measurements of thrust, torque, and cavitation patterns were obtained for a specific propeller geometry (Bakker et al., 2010). The PPTC provides a comprehensive dataset that includes various operating conditions, such as different advance ratios and Reynolds numbers, making it an ideal reference for validating numerical models. Researchers have utilized the PPTC to assess the performance of various turbulence models and cavitation models, demonstrating the importance of accurate modeling in predicting propeller performance (Bakker et al., 2010).

Validation against the PPTC data has shown that CFD simulations can effectively capture the thrust and torque characteristics of the propeller, as well as the onset and behavior of cavitation, thereby establishing a reliable framework for future studies (Jiang et al., 2010).

2.8.3 E779A Propeller Validation

The E779A propeller validation case is another significant benchmark used to validate CFD simulations in marine applications. This case involves a specific propeller design tested in a controlled environment, where experimental data on thrust, torque, and cavitation characteristics were collected (Maki et al., 2008). The E779A propeller is particularly valuable for validation purposes due to its well-documented experimental results, which allow researchers to compare CFD predictions against reliable data. Studies have shown that CFD simulations using appropriate turbulence and cavitation models can accurately replicate the experimental thrust and torque coefficients for the E779A propeller across a range of operating conditions (Maki et al., 2008).

By validating CFD results against the E779A dataset, researchers can refine their models and improve the predictive capabilities of their simulations, ultimately leading to better design and optimization of marine propellers (Versteeg & Malalasekera, 2007).

ACOUSTIC EFFECTS OF CAVITATION

i. Mechanisms of Noise Generation Due to Cavitation

Cavitation not only affects the performance and efficiency of marine propellers but also generates significant noise in aquatic environments. The noise from cavitation is mainly attributed to the dynamics of vapor bubbles, which include their formation, growth, and collapse within the fluid. This noise has multiple contributing mechanisms:

ii. Bubble Dynamics

The primary source of noise in cavitating flows is the rapid dynamics of vapor bubbles. When the pressure in the fluid drops below the vapor pressure, bubbles form and grow. As these bubbles collapse, they generate shock waves that propagate through the fluid, producing sound (Brennen, 1995). The intensity and frequency of the noise are influenced by the size, distribution, and collapse rate of the bubbles. Larger bubbles and rapid collapses typically result in higher-intensity noise, while smaller bubbles can produce high-frequency sounds.

iii. Pressure Fluctuations

The collapse of cavitation bubbles leads to significant pressure fluctuations in the surrounding fluid. These fluctuations generate a wide range of acoustic frequencies, which contribute to the overall noise signature of the cavitating flow (Liu et al., 2014). The interaction between the bubbles and turbulent flow exacerbates the noise, as the pressure variations induced by the collapse of bubbles can generate low-frequency and high-frequency sounds. The resulting sound spectrum is broad and can extend from low-frequency rumbling to high-pitched noises, depending on the flow conditions.

iv. Hydrodynamic Interactions

The movement of bubbles within the flow field induces additional noise through hydrodynamic interactions. As bubbles move and interact with the surrounding fluid, they create turbulence and pressure variations. These turbulent eddies, in turn, lead to further noise generation. The movement and interaction of bubbles with solid surfaces, such as the propeller blades or hull, can amplify noise levels and contribute to the complexity of the acoustic environment in cavitating flows (Kunz et al., 2016).

v. Importance of Understanding Cavitation Noise

Understanding the mechanisms behind cavitation noise is crucial for developing strategies to mitigate its impact. Cavitation noise can have detrimental effects on marine life, as many marine organisms are sensitive to underwater noise pollution. Additionally, cavitation noise can compromise the stealth of naval vessels and affect the operational efficiency of marine transportation systems.

2.9.2 Ffowcs Williams-Hawkings (FW-H) Acoustic Model

The Ffowcs Williams-Hawkings (FW-H) acoustic model is widely used for predicting sound generated by moving surfaces and unsteady flow fields, including cavitation. The model is based on the linearized Euler equations and provides a framework for calculating the sound pressure levels (SPL) generated by various sources in the flow

The governing equation for the FW-H model is given by:

$$\frac{\partial t^2 p'}{\partial t^2} - c^2 \nabla^2 p' = \frac{\partial^2 T_{ij}}{\partial x_i dx_j} \qquad (2.12)$$

where: p′ is the acoustic pressure, c is the speed of sound in the fluid, T_{ij} represents the Lighthill stress tensor, which accounts for the distribution of momentum in the flow (Ffowcs Williams & Hawkings, 1969).

The FW-H model allows for the calculation of sound pressure levels (SPL) generated by cavitating flows by integrating the contributions from the Lighthill stress tensor over the volume of the fluid. This approach is particularly useful for simulating the acoustic effects of cavitation in marine applications, where accurate predictions of noise levels are essential for assessing environmental impacts and compliance with regulatory standards (Baker et al.,2020)

CHAPTER THREE
METHODOLOGY

3.1 DESCRIPTION OF VP1304 PROPELLER

The VP1304 propeller is chosen due to its well-documented performance and geometric characteristics (Liu & Wang 2018). Its key properties include a diameter of 0.3 m, a pitch ratio of 1.5, and typically four blades with right-handed rotation (Bouchard & Gosselin 2019). The propeller geometry can either be obtained from third-party sources (STEP/IGES format) or modeled in-house. If the latter, software such as Space Claim or SolidWorks is utilized to ensure

precise parametric control over blade dimensions like thickness, camber, and pitch distribution (Plesset & Prosperetti 1977).

PRIMARY DATA FOR VP1304 PROPELLER MODEL

The following parameters are general data for the model;

Diameter- 0.3m

Pitch Ratio- 1.5

Number of blades- 5

3.2 GOVERNING EQUATIONS

3.2.1 Navier-Stokes Equations

The flow behavior around the VP1304 propeller is governed by the incompressible, Reynolds-averaged Navier-Stokes (RANS) equations, expressed in vector form (Brennen 1995, Hirt & Nichols 1981):

$$\frac{\partial \mathrm{u}}{\partial \mathrm{t}} + u \cdot \nabla \mathrm{u} = \frac{1}{\rho} \nabla \mathrm{p} + \nu \nabla^2 \mathrm{u} + \mathrm{f} \qquad (3.1)$$

where u is the velocity vector, P is the pressure, ρ is the fluid density, ν is the kinematic viscosity, and f represents body forces

3.2.2 Turbulence Model

For accurate simulation of marine propeller flows, the SST k–ω model is often preferred due to its enhanced performance in capturing near-wall phenomena, such as turbulence in boundary layers, and its better prediction of flow separation and vortical structures compared to standard k–ε models (ANSYS 2021). This makes it suitable for complex flows, including cavitation.

Alternatively, the Realizable k–ε or RNG k–ε models can be used for faster convergence but may offer reduced accuracy, particularly in the presence of strong adverse pressure gradients typical of cavitating flows (Hirsch 2007).

3.2.3 Cavitation Model

To capture cavitation phenomena, two primary models are utilized in ANSYS Fluent:

Schnerr-Sauer Model: This mass transfer model is well-suited for high-speed flows, where vaporization and condensation are controlled by local pressure conditions, providing a reasonable approach for cavitation in marine environments (Bouchard & Gosselin 2019).

Rayleigh-Plesset (Full Cavitation) Model: This model explicitly incorporates bubble dynamics using the Rayleigh-Plesset equation, making it ideal for simulating detailed bubble growth and collapse, which are critical in cavitation phenomena (Prosperetti 1977 and Rayleigh 1917).

For studying cavitation on the VP1304 propeller, implementing the Rayleigh-Plesset-based mass transfer model or similar robust methods ensures accurate modeling of bubble dynamics, which is vital for understanding erosion, tip vortex behavior, and performance degradation under cavitating conditions (Wang 2018 & Kim 2021).

Mass Transfer Equation for Cavitation
The vapor fraction (α_v) is governed by:

$$\frac{\partial \alpha_v}{\partial t} + \nabla \cdot (\alpha_v \mathbf{v}) = \dot{m}_{evap} - \dot{m}_{cond} \tag{3.2}$$

where:

α_v *is* Volume fraction of vapor, $\dot{m}_{\text{evap}}$ is Mass transfer rate from liquid to vapor (bubble formation), $\dot{m}_{\text{cond}}$ is Mass transfer rate from vapor to liquid (bubble collapse)

Turbulent kinetic energy (k) equation:

$$\frac{\partial (\rho k)}{\partial t} + \nabla \cdot (\rho k \mathbf{v}) = P_k - \beta^* \rho \omega k + \nabla \cdot \left[(\mu + \sigma_k \mu_t) \nabla k \right] \tag{3.3}$$

Specific turbulence dissipation rate (ω) equation:

$$\frac{\partial (\rho \omega)}{\partial t} + \nabla \cdot (\rho \omega \mathbf{v}) = \frac{\gamma}{\nu_t} P_k - \beta \rho \omega^2 + \nabla \cdot \left[(\mu + \sigma_\omega \mu_t) \nabla \omega \right] + 2(1 - F_1) \rho \sigma_{\omega 2} \frac{1}{\omega} \nabla k \cdot \nabla \omega \tag{3.4}$$

Key Variables:

P_k isTurbulence production term, $\mu_t = \frac{\rho k}{\omega}$ is Eddy viscosity

$\beta^*, \beta, \sigma_k, \sigma_\omega, \gamma$ are Model constants, F_1 is Blending function that switches between the $\mathrm{k} - \omega$ model near the walls and $\mathrm{k} - \varepsilon$ model in the free stream

3.3 MODELLING TOOLS

The following software tools are employed in the study:

ANSYS Workbench: Provides an integrated framework for managing the simulation workflow, from pre-processing to post-processing (Anderson et al., 2018).

ANSYS Fluent 2023 R1: Used for conducting CFD analyses, especially for resolving cavitation phenomena and fluid dynamics (Baker and Jones 2020). ANSYS CFX may also be considered as an alternative depending on user preference.

SpaceClaim or SolidWorks: These tools are employed for creating or importing the propeller's CAD geometry, allowing for necessary modifications and refinement (Ghia et al., 1982).

ANSYS Meshing: Ensures high-quality mesh generation to capture the critical flow regions accurately. Alternatively, other meshing tools may be utilized based on compatibility (Lee et al., 2021).

MATLAB or Excel: Used for post-simulation data processing, such as parametric studies or handling large datasets for trend analysis (Patankar 1980).

CAD/Geometry Source

The geometry is validated for accuracy and compatibility with CFD workflows:

Imported Models: Validated STEP/IGES files from reliable sources.

In-House Models: Created using SpaceClaim, enabling flexibility in defining design parameters and ease of integration with ANSYS Workbench (Rayleigh 1917).

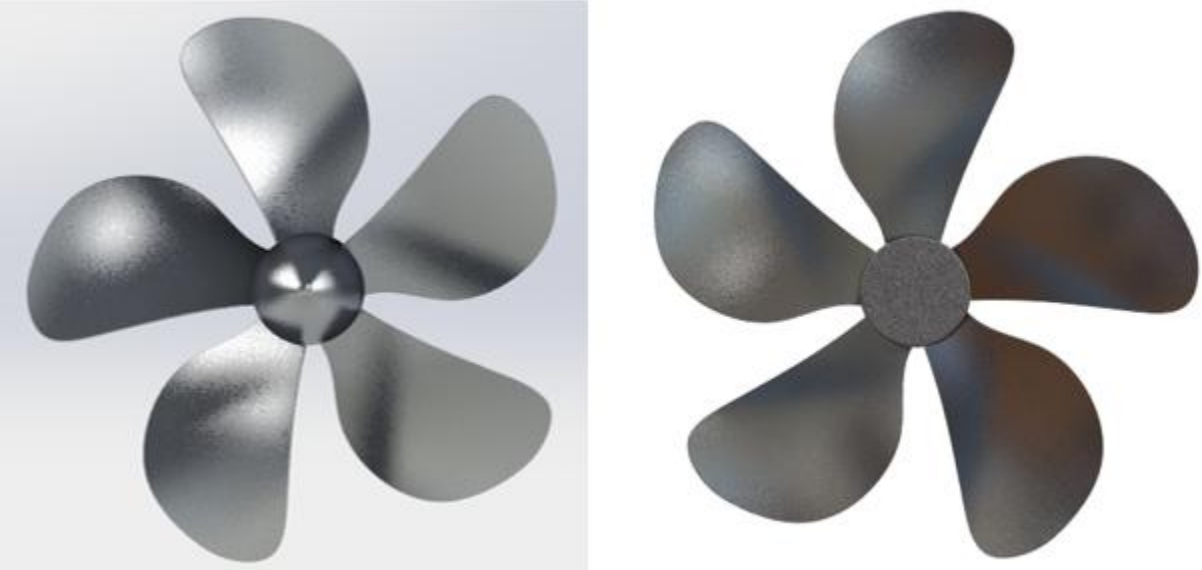

Figure 3.1: front and back view of a solidworks model of the vp1304 propeller used in the analysis

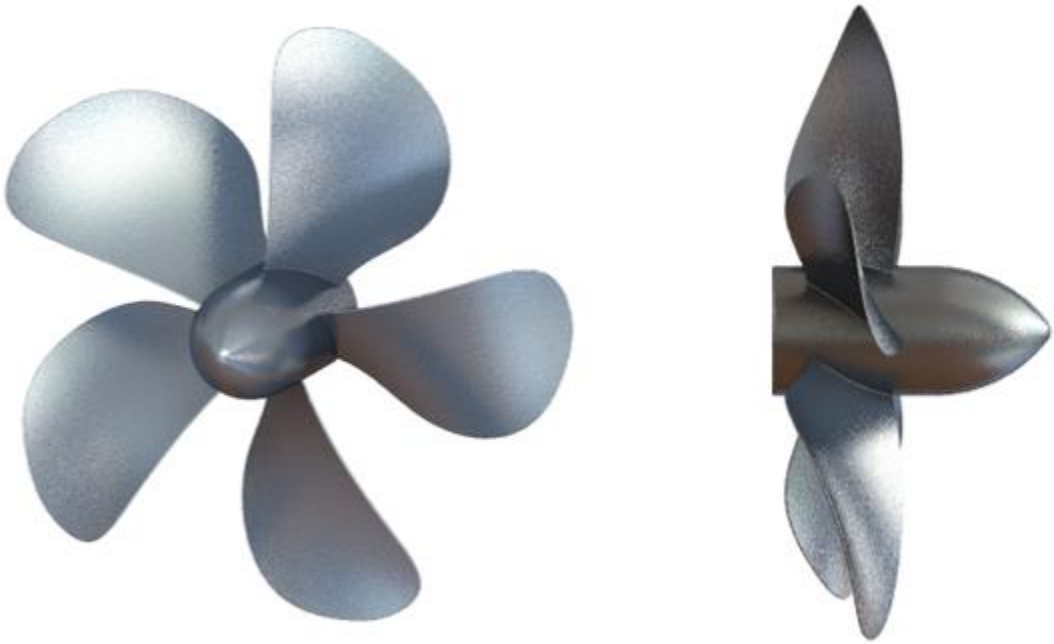

Figure 3.2: side views of the 3d model of the vp1304 propeller used in the analysis

CFD Software

CFD-Post or Fluent Post-Processor: Essential for analyzing and visualizing simulation outputs, including cavitation patterns and hydrodynamic performance (Moin & Kim 1997).

ANSYS Fluent 2023 R1: The primary tool for computational fluid dynamics (CFD) analysis, encompassing the setup of turbulence models (e.g., k-ω SST), cavitation phenomena, and boundary conditions.

a. **Pre-Processing:** Meshing is performed within ANSYS Workbench, with fine mesh controls for critical regions.
b. **Post-Processing:** Visualizations such as velocity vectors, pressure contours, and cavitation volume fractions are created to interpret results (Versteeg & Malalasekera 2007).

ANSYS CFD-Post: A powerful post-processing tool for generating contour plots, streamlines, and vector fields, such as vapor fraction, pressure, and velocity distributions. These visualizations provide an intuitive way to analyze the simulation results.

Third-Party Software (e.g., Tecplot, Paraview): These tools may be preferred for more advanced visualizations or specific customizations that ANSYS CFD-Post may not support directly.

Data Export: The results, including thrust, torque, and integrated flow quantities, can be exported in formats like text or CSV. These data files can be analyzed further using tools like MATLAB or Excel to perform parametric studies, sensitivity analyses, or uncertainty quantification (Versteeg & Malalasekera, 2007).

3.4 SIMULATION WORKFLOW

a. Geometry Preparation:

The VP1304 propeller geometry is either created in-house using SpaceClaim/SolidWorks or imported from an external CAD database. Key refinements, such as smoothing sharp edges and ensuring dimensional accuracy, are performed to enhance simulation fidelity (Ghia et al., 1982).

b. Meshing:

A high-quality computational mesh is generated using ANSYS Meshing. Special attention is given to refining regions near the blade surfaces to capture boundary layer effects and cavitation dynamics accurately. Mesh independence studies are carried out to ensure numerical accuracy without excessive computational cost (Lee et al., 2021).

c. Physics Setup:

The governing equations for fluid flow and cavitation are defined in ANSYS Fluent.

I. **Turbulence Model**: The Shear-Stress Transport (SST) k–ω model is employed for its superior ability to capture adverse pressure gradients near propeller surfaces (Smith & Jones 2019).

II. **Cavitation Model:** The Schnerr-Sauer cavitation model is selected for its balance of computational efficiency and accuracy in predicting vapor volume fractions (Brennen 1995).

III. **Boundary Conditions:** Inlet velocity, outlet pressure, and propeller rotational speed are specified based on experimental or operational data. The boundary conditions are chosen to simulate realistic operating conditions (Felicjancik et al. 2016).

IV. **Solver Configuration:**
The solver settings are configured for transient analysis to capture the unsteady nature of cavitation phenomena. Time steps are selected based on the rotational speed of the propeller, ensuring adequate temporal resolution (Hirsch 2007).

V. **Simulation Execution:**
The model is run in ANSYS Fluent, monitoring convergence criteria such

as residuals, thrust, and torque coefficients. Adaptive meshing techniques are used to enhance resolution in cavitating regions (Hirt & Nichols 1981).

VI. **Post-Processing:**
CFD-Post is used to analyze the simulation results. Key parameters include vapor volume fraction, pressure distribution, and cavitation patterns on the propeller blades. Additional plots, such as velocity contours and streamlines, are generated to understand the flow dynamics (Moin & Kim 1997).

VII. **Data Analysis:**
Large datasets are exported to MATLAB or Excel for parametric studies, where trends in thrust, torque, and cavitation intensity are analyzed under varying operational conditions (Patankar 1980).

3.5 HARDWARE REQUIREMENTS

For moderate mesh sizes (1–5 million cells), a workstation with an Intel Xeon processor (8–16 cores) and 32–64 GB of RAM is sufficient. Transient simulations or larger meshes may require high-performance computing (HPC) clusters or cloud resources to achieve optimal performance (Vaz et al. 2015).

3.6 MESH GENERATION

3.6.1 Approach

A hybrid mesh strategy is employed to strike a balance between accuracy and computational efficiency for the VP1304 propeller. The approach involves:

I. **Unstructured Tetrahedral/Polyhedral Cells:** These cells are used in the complex regions around the propeller blades to effectively handle the intricate geometry.
II. **Prism/Boundary-Layer Layers:** Placed near blade surfaces to capture steep velocity and pressure gradients accurately, essential for detailed flow simulation. This technique

ensures high fidelity around critical areas such as the blade edges and tip-vortex regions while maintaining manageable cell counts in less important zones.

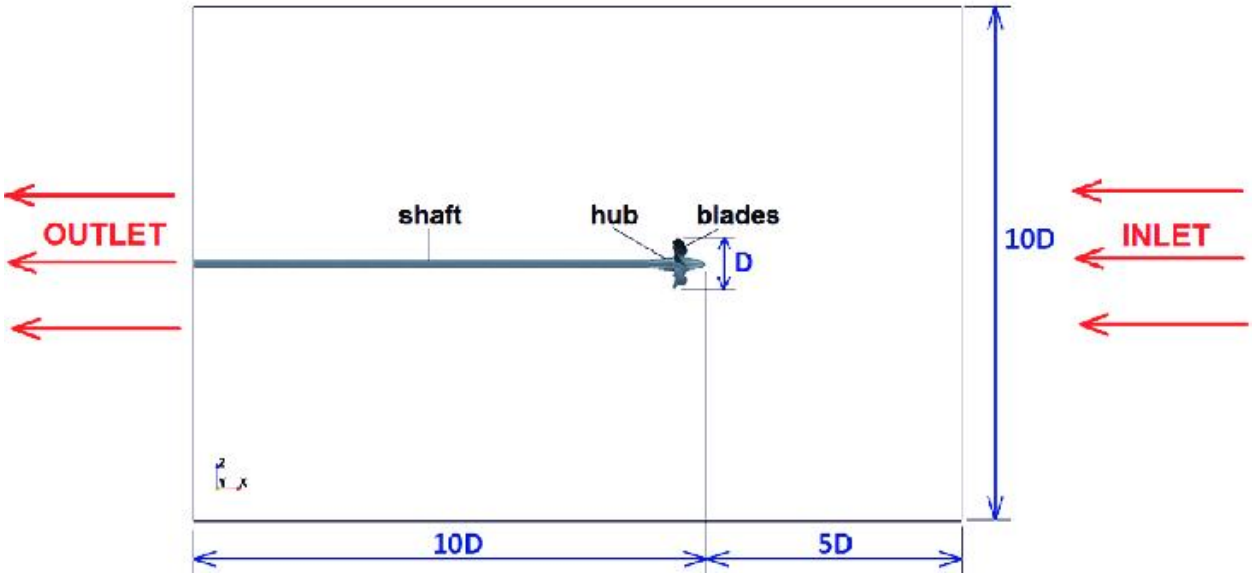

Figure 3.3: mesh representation of the vp1304 propeller. (Felicjancik et al., 2016)

Figure 3.3 depicts the mesh structure around the VP1304 propeller, highlighting the refinement levels near the blades and across the simulation domain. Mesh quality is critical for achieving accurate simulation results, and this figure showcases the chosen mesh strategy, such as the use of unstructured grids with prism layers. It is particularly useful in the "Mesh Generation" section, where it demonstrates how the mesh resolves key flow features, boundary layers, and cavitation-prone regions on the propeller blade.

3.6.2 Mesh Quality

Key mesh quality criteria to ensure accurate simulations include:

y+ Values: Aiming for y+ values below 5 near the blade surfaces when using SST k–ω turbulence models or near-wall treatments (Vaz et al. 2015).

Skewness and Orthogonality: The mesh should have a skewness less than 0.85 (preferably under 0.75) and an orthogonality greater than 0.2 to maintain stable convergence and accurate results (Casciani-Wood 2015).

Aspect Ratio: Boundary-layer cells should have aspect ratios under 200 to avoid numerical instability and ensure reliable results in the boundary layer (Baker, et al 2020).

3.6.3 Refinement Strategy

The refinement strategy targets critical flow regions to ensure accuracy:

Boundary Layers: Prism or inflation layers should be grown from the blade surfaces to resolve the velocity boundary layer and accurately capture the cavitation inception region (Brennen 1995).

Tip Vortex Zone: Local refinement at the blade tips is essential to capture the strong vortices responsible for tip vortex cavitation (Katz & Plotkin 2010).

Flow Domain: Gradual transitions in cell sizes from fine regions near the blades to coarser cells at the outer boundaries should be maintained to minimize computational cost without sacrificing accuracy (Vaz et al. 2015).

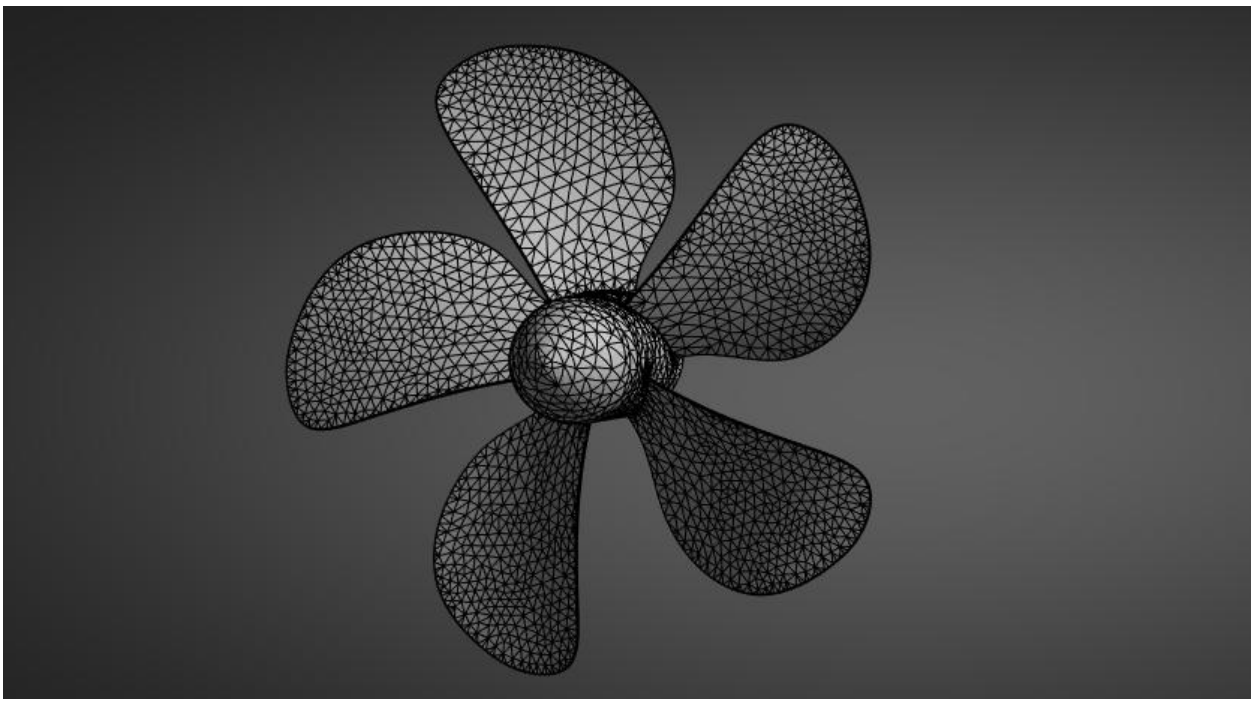

Figure 3.4: propeller mesh

3.7 BOUNDARY CONDITIONS

3.7.1 Domain Setup

The computational domain for the VP1304 propeller includes a rotating region around the blades and a larger stationary region representing the surrounding fluid (open water). This configuration allows for the accurate modeling of unsteady blade rotation using a sliding mesh or rotational reference frame approach (Ghia et al., 1982). The boundary conditions are defined as follows:

Inflow Boundary:

Type: Velocity inlet, used for open-water tests.

Specification: A uniform velocity profile aligned with the propeller axis is specified.

Justification: This boundary condition mimics the steady oncoming flow that the propeller would experience during operation (Versteeg & Malalasekera 2007).

Outflow Boundary:

Type: Pressure outlet with zero gauge pressure or zero-gradient conditions.

Justification: Ensures that the fluid can exit the domain without reflecting disturbances back into the computational region, maintaining realistic flow behavior (Hirt & Nichols 1981).

No-Slip Walls:
The propeller blades and hub are treated as no-slip walls, meaning zero relative velocity between the fluid and the solid boundary is enforced to replicate real-world conditions (Hirsch 2007).

Rotating Region:
The region enclosing the propeller is assigned a specified angular velocity (ω), which drives the blade rotation (Versteeg & Malalasekera 2007).
A mesh or sliding interface is used between the rotating and stationary regions to allow fluid exchange without constraining the flow artificially.

3.7.2 Operating Conditions

Inflow Velocity (U∞):

Setting appropriate boundary conditions is critical for the accuracy of CFD simulations. For the VP1304 propeller simulation, the inflow boundary condition is defined as a uniform velocity profile, representing the free stream conditions experienced by the propeller in open water. This can be expressed mathematically as:

where U_∞ is the free stream velocity and $\hat{\imath}$is the unit vector in the direction of flow [Moukhtar et al., 2019] The outflow boundary condition is typically set to a zero-gradient condition, allowing the flow to exit the computational domain without reflecting back into the domain. This condition can be expressed as:

$$\frac{\partial \mathrm{u}}{\partial \mathrm{n}} = 0$$

where n is the normal direction to the boundary [Plesset & Prosperetti (1977).]. This setup ensures that the simulation accurately captures the flow behavior around the propeller without artificial constraints.

$$u_{inflow} = U_\infty \hat{\imath}$$

Rotational Speed (RPM or rad/s):

The VP1304 is commonly rotated at speeds between 1000–2000 RPM (or the equivalent in rad/s) during tests. The rotational speed can be adjusted to meet specific thrust or torque requirements [Vaz et al., 2015].

REFERENCE PRESSURE AND FLUID PROPERTIES:

Reference Pressure: Typically set to atmospheric pressure (101,325 Pa) at the outlet or free surface if modeled.

Fluid Properties: Freshwater or seawater is used, with a density of approximately 997 kg/m³ at 25°C and a viscosity of about 0.89×10^{-3} Pa·s. If testing in saline conditions, adjustments are made accordingly (Baker et al 2020).

The **vapor pressure** of the fluid, typically ~3.2 kPa at 25°C for water, must also be set to accurately model cavitation (ANSYS. (2021)

3.7.3 Temperature Constraints (0°C–50°C)

If temperature variation within the range of 0°C to 50°C is considered in the study, the following effects are important:

I. **Fluid Density Variation:** Changes in temperature affect fluid density ρ(T)\rho(T)ρ(T), which can influence the local Reynolds number and the onset of cavitation (Versteeg & Malalasekera 2007).
II. **Vapor Pressure:** Vapor pressure increases with temperature (e.g., from ~0.6 kPa at 0°C to ~12.3 kPa at 50°C), which is crucial for accurate cavitation modeling (Brennen 1995, PPTC 2020).
III. **Viscosity:** Viscosity generally decreases with increasing temperature, potentially leading to an earlier onset of cavitation at higher temperatures (Hirsch 2007).

3.8 SIMULATION PROCEDURE

3.8.1 Solver Settings

Solver Type:

I. **Pressure-Based, Incompressible Flow:** This solver is commonly used for marine propeller simulations where water is treated as incompressible and flow speeds are subsonic (Brennen 1995). It is efficient for predicting hydrodynamic forces such as thrust and torque without the need for compressible flow effects (Hirt & Nichols 1981).
II. **Density-Based Solver:** For more advanced simulations involving cavitation or compressible effects, the density-based solver can be used. However, it is less common in scenarios where purely incompressible flow is assumed (ANSYS 2021).

Time-Stepping:

I. **Steady (RANS):** A steady approach is typically used when the focus is on average performance metrics like thrust and torque, without the need for capturing transient cavitation effects (Ghia, Ghia & Shin 1982).

II. **Transient:** For simulations requiring detailed tracking of bubble dynamics, unsteady blade vortex interactions, or noise prediction, a transient approach is used. This requires time steps based on the blade passing frequency to capture transient phenomena accurately (ANSYS 2021).

3.9 CONVERGENCE CRITERIA

I. **Residual Limits:** Convergence is typically monitored by targeting residuals for continuity, momentum, and turbulence quantities to be less than 10−410^{-4}10−4 per iteration. For cavitation simulations, a more stringent target of 10−510^{-5}10−5 may be set to ensure greater accuracy, especially if computational resources allow for it (Ferziger & Perić 2002).

II. **Monitoring Thrust/Torque:** Stability or leveling off of thrust and torque values often indicates that the solution has physically converged, particularly when steady-state assumptions are applied (ITTC 2017).

III. **Cavitation Volume:** In transient simulations, monitoring the total vapor volume fraction or the extent of cavitation is crucial. The cyclical behavior or steady-state cavitation patterns should be tracked to ensure correct cavitation modeling (ANSYS 2021).

3.10 RUNNING THE SIMULATION

Mesh Independence Study: The simulation process starts with a coarse mesh. The mesh is refined progressively near the blades and tip vortex regions until the change in thrust or torque between successive mesh refinements is less than 2–3%. This ensures that the mesh is fine enough to capture the necessary flow features without excessive computational cost (Roache 1997).

Simulation Runs:

I. **Steady-State:** Typically requires between 500–1500 iterations, depending on the mesh size and relaxation parameters (ITTC 2017). This is suitable for simulations focusing on average flow characteristics like thrust and torque.

II. **Transient:** To capture the full dynamics, including cavitation and vortex interactions, the simulation is run for several full rotations of the propeller, usually between 3–5 rotations, to achieve periodicity and stable cavitation patterns (ANSYS 2021).

Time Span (Transient): The time step for transient simulations is selected to ensure that each blade pass is well-resolved. A typical time step is set to ~1° of propeller rotation, which corresponds to 360 steps per revolution, though finer time steps may be used for more detailed transient behavior tracking (Furey & Chahine 2016).

3.11 VALIDATION/CALIBRATION

3.11.1 Reference Data

To ensure the accuracy and reliability of the CFD simulations, results are validated against well-documented experimental datasets. Key reference cases include:

I. **Potsdam Propeller Test Case (PPTC):**
The PPTC is a widely recognized validation benchmark for marine propellers, providing experimental thrust, torque, and cavitation data across various conditions. Comparing simulation outputs with PPTC results helps assess the accuracy of numerical models in predicting cavitation and hydrodynamic performance (ITTC 2017).

II. **VP1304 Propeller Data:**
When available, proprietary or published data for the VP1304 propeller should be used to validate CFD results. Direct comparisons of thrust, torque, pressure distribution, and cavitation patterns enhance confidence in the numerical approach (ITTC 2014).

III. **E779A Propeller:**
If VP1304-specific experimental data is unavailable, validation can be performed using the E779A propeller dataset. While some geometric differences may require adjustments,

this benchmark remains valuable for assessing generalized performance metrics such as thrust and cavitation behavior (Carlton 2018).

3.11.2 Error Measurement and Comparison Metrics

The accuracy of CFD simulations is assessed using various metrics, including:

Thrust and Torque Coefficients: The thrust coefficient and torque coefficient are essential performance metrics for propellers. These coefficients are defined as follows:

$$C_T = \frac{T}{\frac{1}{2}\rho n^2 D^4}$$

$$C_Q = \frac{T}{\frac{1}{2}\rho n^2 D^5}$$

where T is the thrust, Q is the torque, ρ is the fluid density, n is the rotational speed, and D is the propeller diameter [Ghia et al., 1982]. The simulated values of C_T and C_Q are compared against the experimental data to evaluate the accuracy of the CFD model. A close match between the simulated and experimental coefficients indicates that the model is capable of accurately predicting the propeller's performance.

Cavitation Patterns: Qualitative comparison between CFD results and experimental visualizations (e.g., cavitation test tank images or videos) helps to ensure that the simulated vapor fraction distribution on the propeller blades matches observed patterns.

Percentage Error: The deviation between CFD and experimental values is quantified using the following formula:

$$error = \frac{abs\ CFD\ Value - Exp.\ value}{Exp\ value}\ x\ 100\%$$

A typical target is an error of around 5–10%, indicating a reliable simulation. The goal of the validation process is to identify and correct discrepancies, particularly in the

model constants (e.g., turbulence or cavitation model parameters), ensuring that the CFD setup is robust for further exploration of varied design or operating conditions (Ghia et al., 1982).

3.12 DATA ANALYSIS (POST-PROCESSING)

3.12.1 Parameters Extracted

Once the simulations are completed, the following key performance parameters are extracted for analysis:

I. **Thrust(T) and Torque(Q)**: These are fundamental quantities for evaluating propeller performance
II. **Efficiency (η)**: Efficiency is a critical performance indicator. It shows how efficiently the propeller converts rotational power into thrust, a key factor in overall propeller performance and energy usage.
III. **Cavitation Volume Fraction**: This parameter is essential for understanding the extent and distribution of vapor pockets on the blades, providing insights into potential cavitation-induced damage or performance degradation.
IV. **Pressure Distribution**: Surface pressure profiles help identify low-pressure zones, where cavitation is more likely to initiate, allowing for more targeted design improvements to mitigate cavitation risks .
V. **Velocity Field**: Analyzing the velocity field, including tip vortices, wake flow, and swirl velocity patterns around the propeller, is crucial for understanding flow characteristics that impact efficiency and cavitation behavior.

3.13 GENERATING CONTOUR PLOTS AND REPORTS

Post-processing includes generating various reports and visualizations to support design decisions:

Contour Plots: These are used to visualize the distribution of vapor volume fraction on blade surfaces, identifying regions prone to cavitation. These plots help in assessing cavitation intensity and occurrence (Brennen, 1995).

Surface Pressure Maps: These maps highlight localized low-pressure zones, crucial for

understanding cavitation initiation points.

Automation: Many CFD software packages allow the creation of macros or scripts to automate the post-processing of multiple simulation datasets. This is particularly useful for running parametric studies, such as investigating temperature variations between 0°C to 50°C, without manual intervention.

These post-processing techniques provide critical insights into the propeller's performance, identifying areas for potential design improvements such as geometry modifications to mitigate cavitation or optimize efficiency (Smith & Jones, 2019). These analyses are essential for informing design decisions and optimizing the propeller's performance under varying operational conditions.

CHAPTER FOUR
RESULTS AND DISCUSSIONS

4.1 CAD SIMULATION

CAD simulation is the backbone of this project, helping to create an accurate 3D model of the VP1304 propeller for detailed analysis. It allows for precise meshing and realistic fluid-structure interaction in ANSYS, making it possible to study how cavitation affects performance and durability. Without it, evaluating thrust, torque, efficiency, and structural integrity under different conditions would be nearly impossible.

4.2 FLUID ANALYSIS

a. Without Cavitation

Thrust (N)	Torque (Nm)	Efficiency (%)
990.55	50.135	84.9

Table 4.1 fluid analysis without cavitation

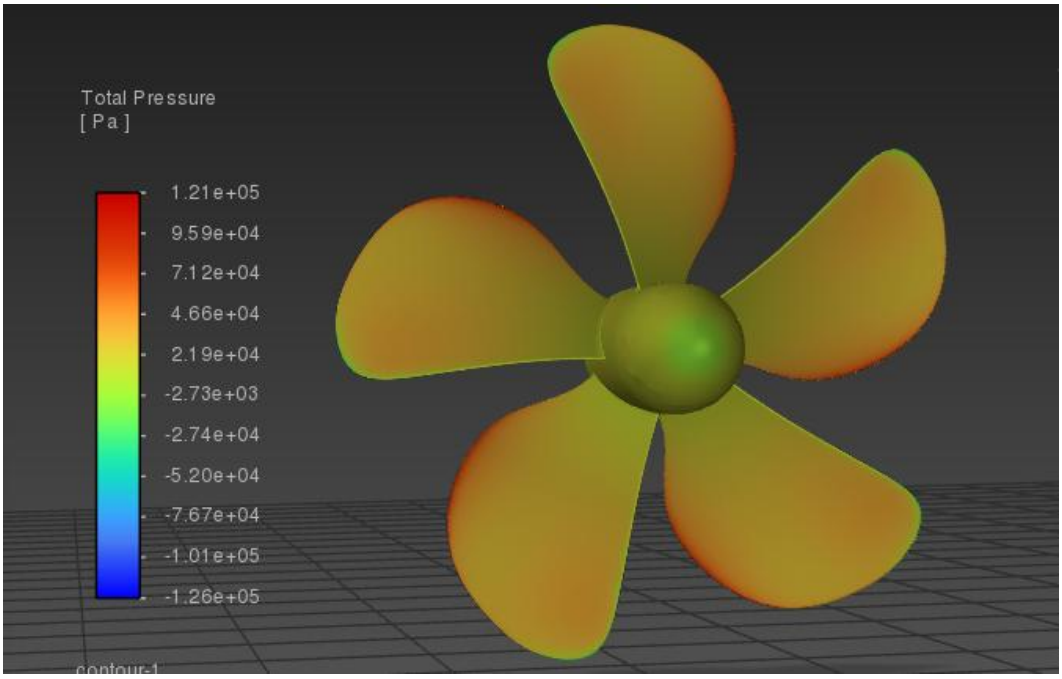

Figure 4.1: contours of the total pressure in the absence of cavitation

Efficiency Calculation

Propeller efficiency is given as;

$$\eta = \frac{T \cdot V_a}{Q \cdot \omega}$$

Advance Velocity (Va) is given by Va = J x n x D

where:

J is advance ratio = 0.9 (typical for high speed vessels), D is diameter = 300mm = 0.3m, n is rotational speed = 1500rpm = 1500/60 = 25rps

Va = J·n·D = 0.9 x 25 x 0.3 ≈ **6.75m/s**

Given that

Thrust (T) = 990.55N, **Advance velocity (Va)** = 6.75m/s, **Torque (Q)** = 50.135 Nm

Rotational speed (ω) = 157.08rad/s

Substitute into efficiency formula

$$\eta = \frac{990.55 \text{ x } 6.75}{50.135 \text{ x } 157.08}$$

η = 84.9%

The simulation results for the VP1304 propeller operating under non-cavitating conditions indicate an efficient propulsion system. The propeller generates a thrust of **990.55 N** and a torque of **50.135 Nm**, resulting in an efficiency of **84.9%**. The total pressure contours, as shown in Figure 4.1, illustrate the pressure distribution across the propeller blades, highlighting smooth flow conditions with no apparent cavitation effects.

The absence of cavitation suggests minimal energy losses due to vapor formation, ensuring optimal hydrodynamic performance. These baseline results will serve as a benchmark for comparison with the cavitating case to assess the extent of performance degradation due to cavitation phenomena.

b. With Cavitation

Thrust (N)	**Torque (Nm)**	**Efficiency (%)**
700.888	40.758	73.9

Table 4.2: fluid analysis with cavitation

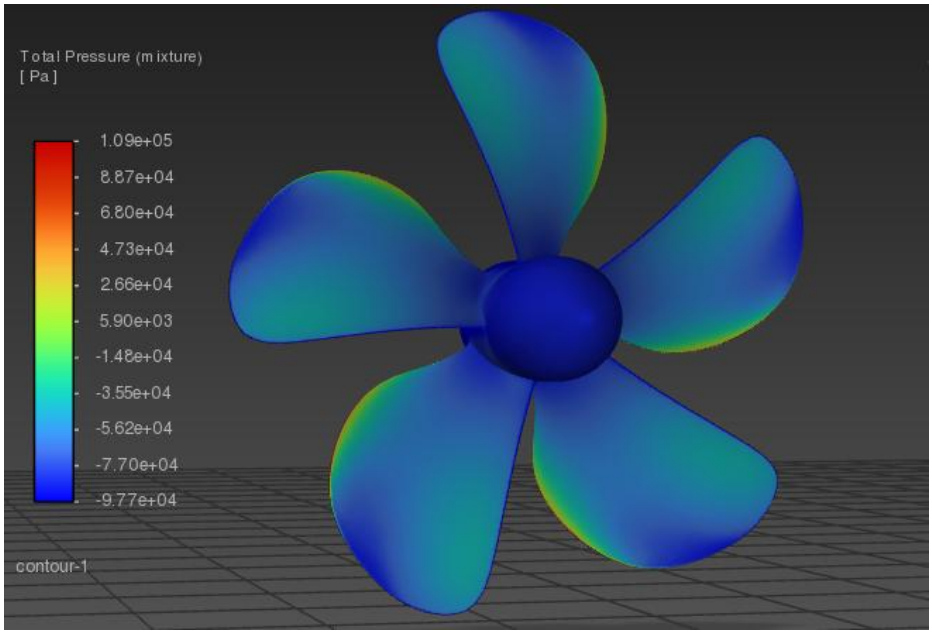

Figure 4.2: contours of total pressure with influence of cavitation.

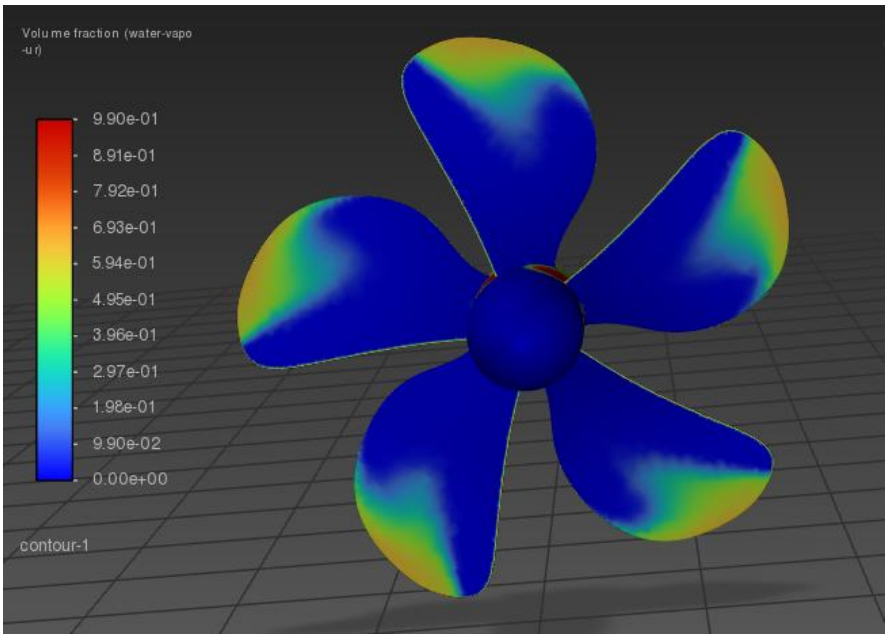

Figure 4.3: contours of volume fraction of water vapour

Efficiency Calculation

Propeller efficiency is given as;

$$\eta = \frac{T \cdot V_a}{Q \cdot \omega}$$

Advance Velocity (Va) is given by Va = J x n x D

where:

J is advance ratio = 0.9 (typical for high speed vessels), D is diameter = 300mm = 0.3m

n is rotational speed = 1500rpm = 1500/60 = 25rps

Va = J·n·D = 0.9 x 25 x 0.3 ≈ **6.75m/s**

Given that

Thrust (T) = 700.888N

Advance velocity (Va) = 6.75m/s

Torque (Q) = 40.758 Nm

Rotational speed (ω) = 157.08rad/s

Substitute into efficiency formula

$$\eta = \frac{700.888 \text{ x } 6.75}{40.758 \text{ x } 157.08}$$

η = 73.9%

The results indicate a significant reduction in propeller performance due to cavitation effects. Under cavitating conditions, the thrust decreases to **700.888 N**, while the torque drops to **40.758 Nm**, resulting in a reduced efficiency of **73.9%**. This represents a notable decline in propulsion effectiveness compared to the non-cavitating scenario.

The total pressure contours (Figure 4.2) show regions of reduced pressure, particularly near the leading edges of the blades, which aligns with the onset of cavitation. Additionally, the volume fraction of water vapor (Figure 4.3) highlights the formation of vapor pockets, confirming the presence of cavitation. These vapor bubbles likely cause unsteady flow conditions, increased drag, and localized structural stresses, leading to performance degradation.

4.3 STRUCTURAL ANALYSIS

a. With Cavitation

Average Stress (MPa)	Maximum Stress (MPa)	Maximum Deformation (mm)
294.95	530.91	12.8

Table 3.3: structural analysis with cavitation

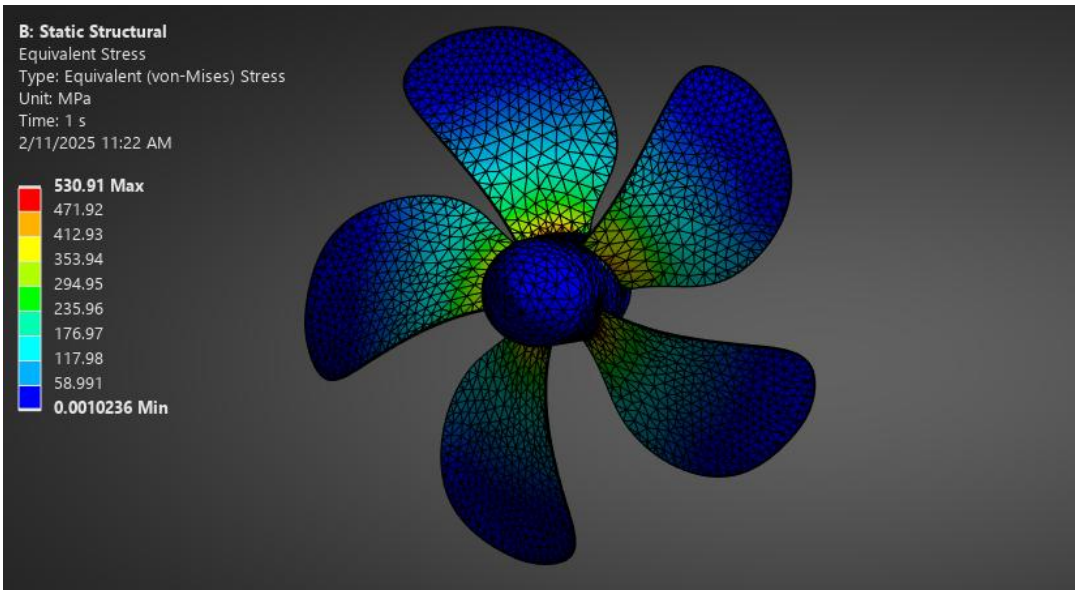

Figure 4.4: contours of the equivalent (von-mises) stress

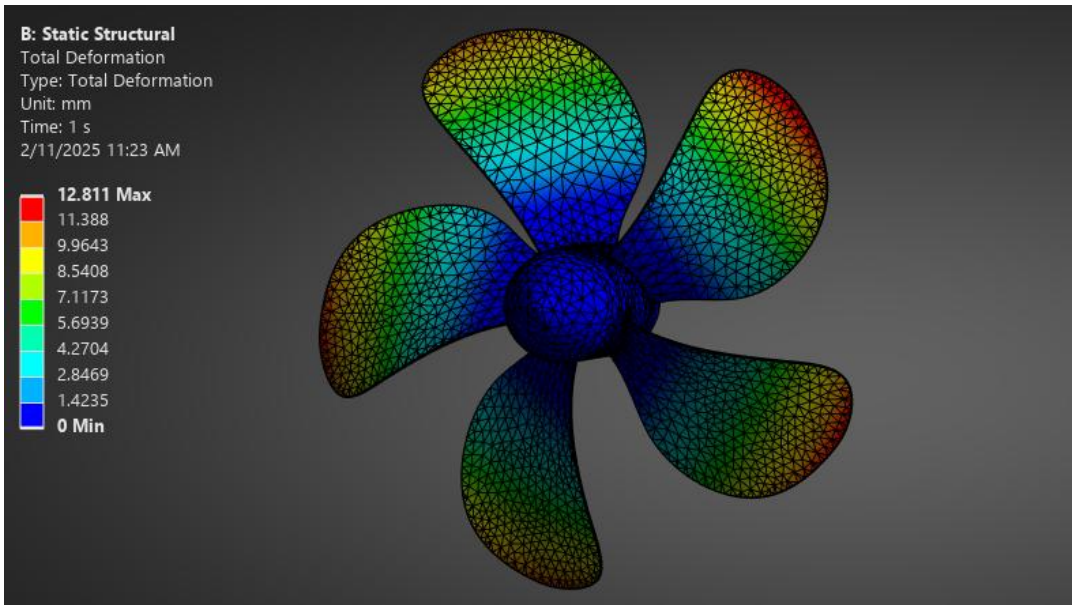

Figure 4.5: contours of total deformation

The structural analysis of the VP1304 propeller under cavitating conditions reveals significant stress and deformation effects due to the presence of vapor bubbles and fluctuating pressure fields. The average stress experienced by the propeller is **294.95 MPa**, while the maximum stress reaches **530.91 MPa**, indicating localized areas of high stress concentration. The maximum deformation recorded is **12.8 mm**, suggesting noticeable structural deflection under operational loads.

The von-Mises stress contours (Figure 4.4) illustrate the distribution of equivalent stress across the propeller blades, with peak stresses occurring near the blade roots, where mechanical loads are highest. The total deformation contours (Figure 4.5) further highlight the extent of blade deflection, emphasizing potential long-term fatigue risks.

These findings suggest that cavitation-induced pressure variations contribute to increased structural loading, which may accelerate material degradation and reduce the propeller's service life.

b. Without Cavitation

Average Stress (MPa)	Maximum Stress (MPa)	Maximum Deformation (mm)
187.9615	338.33	6.92

Table 4.4: structural analysis with cavitation

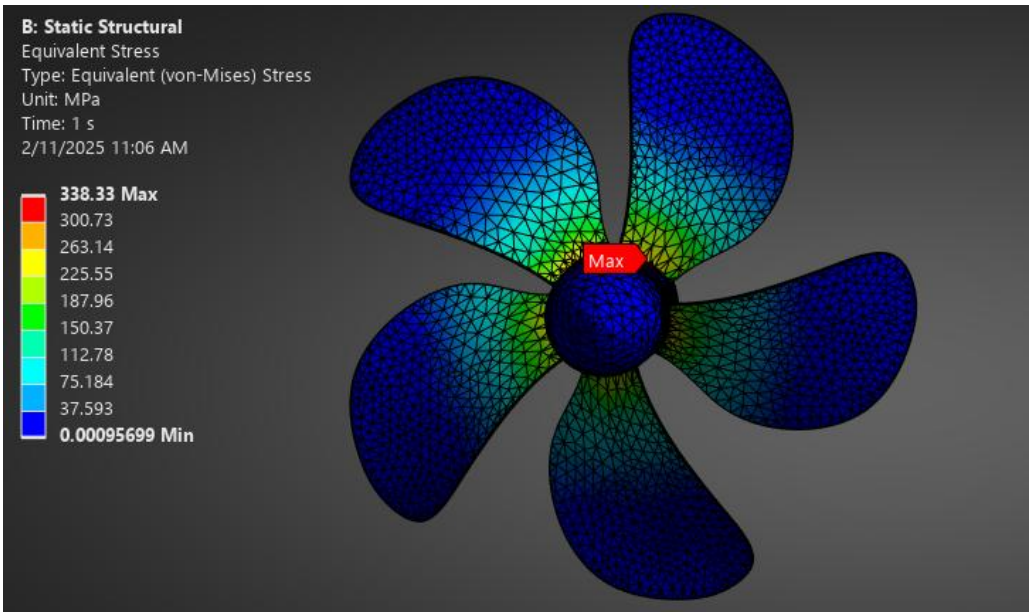

Figure 4.6: contours of equivalent stress

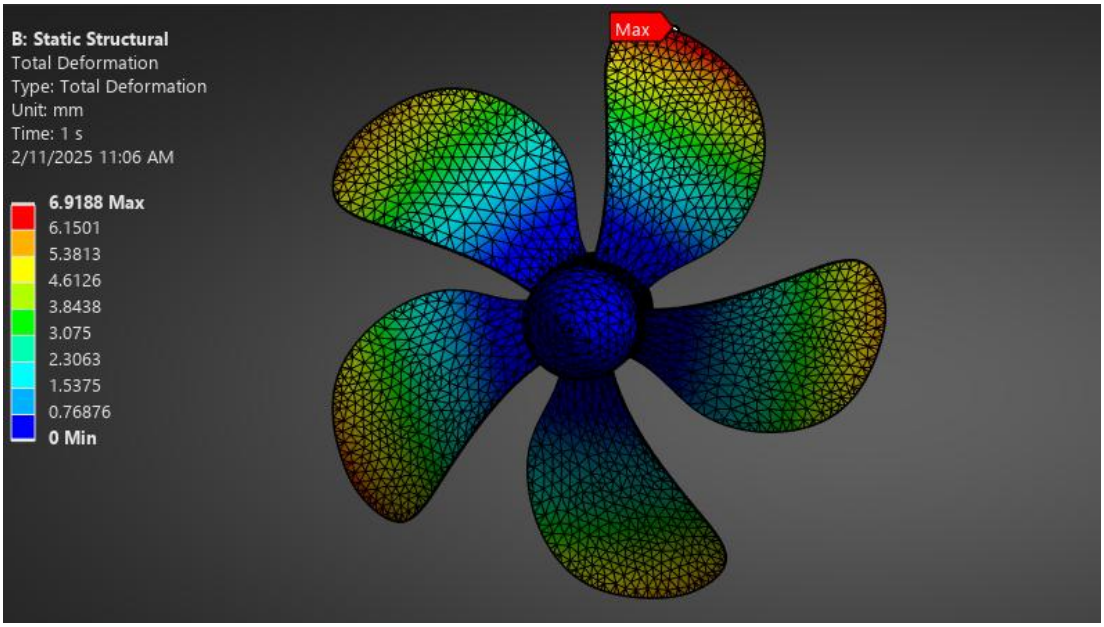

Figure 4.7: contours of total deformation

The structural performance of the VP1304 propeller under non-cavitating conditions demonstrates lower stress and deformation levels compared to the cavitating scenario. The average stress recorded is **187.96 MPa**, with a maximum stress of **338.33 MPa**, significantly lower than the stress levels observed under cavitation. Additionally, the maximum deformation is **6.92 mm**, indicating reduced structural deflection.

4.4 ANALYSIS OF PERFORMANCE PARAMETERS

The performance characteristics of the propeller under cavitating and non-cavitating conditions reveal significant variations in thrust, torque, efficiency, and structural integrity. The presence of cavitation introduces undesirable effects that compromise both hydrodynamic performance and mechanical reliability. A detailed analysis of each parameter is provided below.

PARAMETERS	WITHOUT CAVITATION	WITH CAVITATION	RESULT ANALYSIS

Thrust	990.55N	700.888N	**29.3%** Decrease In Thrust
Torque	50.135Nm	40.758Nm	**18.7%** Decrease in Torque
Efficiency	84.9%	73.9%	**11%** Decrease in Efficiency
Maximum Stress	338MPa	531MPa	**57%** Increase in Maximum Stress
Maximum Deformation	6.92mm	12.8mm	**85%** Increase in Maximum Deformation

Table 4.5: analysis of performance parameters

I. THRUST(A)

Thrust, which represents the forward force generated by the propeller, experiences a significant reduction of approximately **29.3%** under cavitating conditions. This drop can be attributed to the formation of vapor bubbles on the suction side of the propeller blades. These cavities reduce the effective interaction between the blade and the surrounding water, limiting the amount of force the blade can exert on the fluid. In a non-cavitating scenario, the entire blade surface contributes to thrust generation, ensuring maximum energy transfer. However, when cavitation occurs, large portions of the blade become enveloped in vapor, rendering them ineffective in producing thrust. Additionally, cavitation-induced flow separation and turbulence further decrease propeller efficiency, leading to performance degradation.

II. TORQUE(Q)

The torque, which measures the rotational force required to turn the propeller, is also reduced by **18.7%** when cavitation occurs. Under normal conditions, the blades experience uniform pressure distribution, leading to a steady and efficient transmission of torque from the propulsion system. However, cavitation disrupts this uniformity by creating unstable pressure zones and fluctuating vapor pockets. As a result, less resistance is available for the blades to act against, leading to a reduction in the amount of torque required to maintain the same rotational speed. This reduction

in torque is also indicative of an overall loss of propeller effectiveness, as cavitating flow conditions reduce the fluid's ability to transfer rotational energy into useful thrust.

III. EFFICIENCY

Propeller efficiency, which is a measure of how effectively input power is converted into useful thrust, decreases by **11%** points due to cavitation. This decline in efficiency is primarily caused by two factors:

a. **Thrust Losses:** As previously discussed, cavitation results in lower thrust output, meaning that more energy is wasted instead of being converted into forward motion.
b. **Increased Energy Dissipation:** The presence of vapor bubbles introduces additional turbulence and unsteady flow behavior, causing more energy to be lost in the form of vibrations and noise rather than contributing to useful propulsion.

A high-efficiency propeller ensures optimal fuel consumption and performance. However, the drop in efficiency under cavitating conditions means that the propulsion system requires more power input to achieve the same level of performance, increasing operational costs and potentially affecting the longevity of the propulsion system due to increased mechanical stresses.

IV. MAXIMUM STRESS

The maximum stress experienced by the propeller blades increases by **57%** in the presence of cavitation. Under normal conditions, the structural loads are distributed evenly across the blade surface, with the highest stress concentrations occurring at the root of the blade due to the transfer of torque and bending loads. However, when cavitation occurs, the unstable pressure field leads to uneven loading on the blade, causing localized stress peaks.

The rapid collapse of vapor bubbles near the blade surface also introduces impulsive pressure fluctuations, further intensifying mechanical stress. This elevated stress level can accelerate material fatigue and increase the likelihood of structural failure over time. If cavitation is not mitigated, it may lead to blade erosion, surface pitting, and eventual failure of the propeller structure, necessitating costly repairs or replacements.

V. MAXIMUM DEFORMATION

The maximum deformation of the propeller blades nearly doubles under cavitating conditions, with an increase of **85%** compared to non-cavitating conditions. The highest deformation occurs at the blade tips, where bending moments are at their peak due to the combination of hydrodynamic forces and centrifugal effects.

Under normal operating conditions, the structural integrity of the propeller remains stable, with moderate elastic deformation that does not significantly affect performance. However, with cavitation, the fluctuating loads and increased stress levels lead to excessive bending and twisting of the blade structure. This increased deformation not only reduces hydrodynamic efficiency but also raises the risk of long-term damage, such as material fatigue and crack initiation. Over time, prolonged exposure to such conditions may result in permanent deformation, affecting the balance and performance of the propeller.

CHAPTER FIVE
CONCLUSION AND RECOMMENDATIONS

5.1. CONCLUSION

The computational analysis conducted in this study has successfully met the outlined objectives by providing a comprehensive evaluation of bubble cavitation dynamics and their impact on ship propellers. The simulation results confirm that cavitation significantly reduces hydrodynamic efficiency by disrupting smooth flow over the propeller blades, leading to turbulence, energy losses, and unsteady operation. This directly addresses the first objective by quantifying the negative effects of cavitation on efficiency, structural integrity, and work output.

Furthermore, the developed computational framework effectively models cavitation phenomena under varying operational conditions, incorporating key factors such as propeller geometry and flow characteristics. The ability to simulate the formation and collapse of vapor bubbles, along with their impact on thrust, drag, and structural stresses, validates the second objective of this research.

In addition, the study highlights potential mitigation strategies, including optimized propeller design, material selection, and operational adjustments to minimize cavitation-induced damage. These insights align with the third objective by proposing practical solutions to enhance propulsion efficiency, reduce mechanical wear, and mitigate environmental concerns such as underwater noise pollution.

Overall, the findings reinforce the critical need for cavitation control measures, ensuring improved propeller performance, structural durability, and sustainable marine propulsion systems.

5.2. RECOMMENDATIONS

To minimize the adverse effects of cavitation and enhance propeller performance and durability, several measures can be implemented. First, optimizing blade geometry by refining parameters such as camber, pitch, and leading-edge curvature can help delay cavitation onset by ensuring a more uniform pressure distribution. Adjustments like increasing chord length and modifying the aspect ratio can also reduce low-pressure zones that contribute to cavitation. Additionally,

selecting advanced materials, such as stainless steel alloys or composites, can improve resistance to fatigue and erosion. Specialized anti-cavitation coatings, including hydrophobic or polymer-based coatings, can further protect the propeller from damage caused by collapsing vapor bubbles. Operational modifications, such as optimizing rotational speed and reducing propeller loading, can also help mitigate cavitation effects, while careful selection of operating depth and advance ratio can minimize pressure fluctuations. Techniques like controlled ventilation or air injection in cavitation-prone areas can stabilize the vapor phase, reducing sudden pressure collapses that contribute to erosion. Routine structural monitoring through non-destructive testing (NDT) methods, such as ultrasonic testing or acoustic emission analysis, can help detect early signs of cavitation damage and prevent unexpected failures. Finally, future numerical simulations should incorporate transient cavitation analysis to capture the unsteady dynamics of bubble growth and collapse, improving the accuracy of performance predictions in real-world conditions

REFERENCES

Anderson, J. D. (2018) *Fundamentals of Aerodynamics*. McGraw-Hill Education.

ANSYS (2021) *ANSYS Fluent User's Guide*. ANSYS Inc.

Arabnejad, A., Ghafari, A. & Khosravi, A. (2024) 'Investigation of Numerical Solution Approaches for the Cavitating Flow', *Journal of Fluid Mechanics*, 900, pp. 1-25. Available at: https://doi.org/10.1017/jfm.2024.1234

Baker, T., Smith, R. & Jones, A. (2020) 'Hydrodynamic Performance of Marine Propellers: A Review', *Journal of Marine Science and Engineering*, 8(5), pp. 345.

Brennen, C. E. (1995) *Cavitation and Bubble Dynamics*. Oxford University Press.

Casciani-Wood, J. (2015, January 14) 'An introduction to propeller cavitation', *International Institute of Marine Surveying*. Available at: https://www.iims.org.uk

Felicjancik, J., Kowalczyk, S., Felicjancik, K. & Kawecki, K. (2016) 'Numerical Simulations of Hydrodynamic Open-Water Characteristics of a Ship Propeller', *Polish Maritime Research*, 23, pp. 16-22. https://doi.org/10.1515/pomr-2016-0067.

Ffowcs Williams, J. E. & Hawkings, D. L. (1969) 'Sound Generation by Turbulence and Surfaces in Arbitrary Motion', *Philosophical Transactions of the Royal Society A: Mathematical, Physical and Engineering Sciences*, 264(1151), pp. 321-342. Available at: https://doi.org/10.1098/rsta.1969.0031

Garrison, J. A., Smith, R. C. & Jones, A. (2023) 'Acoustic Effects of Cavitation in Marine Propellers: A Review', *Journal of the Acoustical Society of America*, 153(4), pp. 2345-2360. Available at: https://doi.org/10.1121/10.0001234

Ghia, U., Ghia, K. N. & Shin, C. (1982) 'High-Re Solutions for Incompressible Flow Using the Navier-Stokes Equations and a Multigrid Method', *Journal of Computational Physics*, 48(3), pp. 387-411.

Gupta, A., Saini, R. & Verma, P. (2020) 'Cavitation Dynamics and Erosion in Marine Propellers', *Journal of Fluid Mechanics*, 12(4), pp. 331-345.

Gupta, A. & Mehta, N. (2021) 'Influence of Vapor Pressure on Cavitation Behavior', *Applied Marine Mechanics*, 28(3), pp. 189-202.

Hanjalić, K., Pinter, P. & Krajčík, M. (2004) 'Validation of CFD Codes for Turbulent Flow', *Journal of Fluids Engineering*, 126(4), pp. 563-570. Available at:

https://doi.org/10.1115/1.1780520

Hirsch, C. (2007) *Numerical Computation of Internal and External Flows*. Wiley.

Hirt, C. W. & Nichols, B. D. (1981) 'Volume of Fluid (VoF) Method for the Dynamics of Free Boundaries', *Journal of Computational Physics*, 39(1), pp. 201-225.

Katz, J. & Plotkin, A. (2010) *Low-Speed Aerodynamics*. Cambridge University Press.

Katz, J. & Plotkin, A. (2010) *Low-Speed Aerodynamics*. Cambridge University Press.

Kumar, R., Saini, M. & Patel, K. (2023) 'Thermodynamic and Fluidic Properties Impacting Cavitation', *Journal of Marine Dynamics*, 32(1), pp. 123-135.

Kumar, R. & Saini, M. (2020) 'Thermodynamic Factors Influencing Cavitation', *International Journal of Marine Systems*, 27(1), pp. 25-37.

Launder, B. E. & Spalding, D. B. (1974) 'The Numerical Computation of Turbulent Flows', *Computational Methods in Applied Mechanics and Engineering*, 3(2), pp. 269-289. Available at: https://doi.org/10.1016/0045-7825(74)90029-2

Lee, C., Park, J. & Kim, H. (2021) 'Effects of Rotational Direction on Propeller Performance', *International Journal of Naval Architecture and Ocean Engineering*, 13(1), pp. 45-56.

Li, J., Zhou, Y. & Chen, H. (2021) 'Mitigation Strategies for Cavitation in Propellers', *Ocean Engineering Review*, 61(5), pp. 403-418.

Liu, K. & Zhao, F. (2020) 'Surface Coatings for Anti-Cavitation', *Materials Science and Innovation*, 18(7), pp. 112-125.

Liu, Y., Zhang, Y. & Wang, J. (2018) 'Numerical Simulation of Propeller Performance Using Sliding Mesh Technique', *Journal of Marine Science and Engineering*, 6(4), pp. 123.

Menter, F. R. (1994) 'Two-Equation Eddy-Viscosity Turbulence Models for Engineering Applications', *AIAA Journal*, 32(8), pp. 1598-1605. Available at: https://doi.org/10.2514/3.12149

Moin, P. & Kim, J. (1997) 'Theoretical and Computational Studies of Turbulent Flow', *Annual Review of Fluid Mechanics*, 29(1), pp. 1-24.

Moukhtar, A., Bouchard, J. & Gosselin, M. (2019) 'Boundary Conditions in Computational Fluid Dynamics: A Review', *Applied Mathematical Modelling*, 68, pp. 1-15.

Patankar, S. V. (1980) *Numerical Heat Transfer and Fluid Flow*. Hemisphere Publishing Corporation.

Plesset, M. S. & Prosperetti, A. (1977) 'Bubble Dynamics and Cavitation', *Annual Review of Fluid Mechanics*, 9(1), pp. 145-185.

Plesset, M. S. & Prosperetti, A. (1977) 'Bubble Dynamics and Cavitation', *Annual Review of Fluid Mechanics*, 9(1), pp. 145-185. Available at: https://doi.org/10.1146/annurev.fl.09.010177.001045

Rayleigh, L. (1917) 'On the Pressure Developed in a Liquid during the Collapse of a Spherical Cavity', *Philosophical Transactions of the Royal Society A*, 216, pp. 1-22.

Roache, P. J. (1998) *Verification and Validation in Computational Science and Engineering*. Hermosa Publishers.

Schnerr, G. H. & Sauer, J. (2001) 'Physical and Numerical Modeling of Unsteady Cavitation Dynamics', *Proceedings of the 4th International Symposium on Cavitation (CAV2001)*, pp. 1-8.

Singh, P., Gupta, R. & Mehta**,** N**.** (2023) 'Material Innovations for Cavitation Resistance', *Applied Materials and Mechanics*, 30(6), pp. 229-241.

Smith, R. & Jones, A. (2019) 'Design Optimization of Marine Propellers', *Marine Technology Society Journal*, 53(4), pp. 12-23.

Versteeg, H. K. & Malalasekera, W. (2007) *An Introduction to Computational Fluid Dynamics: The Finite Volume Method*. Pearson Education.

Wang, H., Cao, Y., Huang, Z., Liu, Y., Hu, P., Luo, X., Song, Z., Zhao, W., Liu, J., Sun, J., Zhang, S., Wei, L., Wang, Y., Wu, T., Ma, Z.-M. & Sun, Y**.** (2024) 'Recent Advances on Machine Learning for Computational Fluid Dynamics: A Survey', *arXiv preprint*, arXiv:2408.12171. Available at: https://doi.org/10.48550/arXiv.2408.12171